

# Continuous time analysis of fleeting discrete price moves

NEIL SHEPHARD

*Department of Economics and Department of Statistics,  
Harvard University  
shephard@fas.harvard.edu*

JUSTIN J. YANG

*Department of Statistics,  
Harvard University  
juchenjustinyang@fas.harvard.edu*

September 18, 2021

## Abstract

This paper proposes a novel model of financial prices where: (i) prices are discrete; (ii) prices change in continuous time; (iii) a high proportion of price changes are reversed in a fraction of a second. Our model is analytically tractable and directly formulated in terms of the calendar time and price impact curve. The resulting càdlàg price process is a piecewise constant semimartingale with finite activity, finite variation and no Brownian motion component. We use moment-based estimations to fit four high frequency futures data sets and demonstrate the descriptive power of our proposed model. This model is able to describe the observed dynamics of price changes over three different orders of magnitude of time intervals.

Keywords: integer-valued stochastic process, Lévy basis, Lévy process, trawl process, market microstructure, realized variance, variance signature plot

## 1 Introduction

Extracting information from the order and trading flow in financial markets is important for trading at high and low frequencies, formulating policy and regulation and studying forensic finance. The distinctness about this area is the frequent focus on the very short term, usually over time intervals which may be much less than a second. At very short time scales, three essential aspects dominate: (i) prices are discrete, due to the tick structure of the market; (ii) prices change in continuous time; (iii) a high proportion of price changes are fleeting, reversed in a fraction of a second. However, the econometricians' cupboard is practically bare, for there are nearly no models or techniques that focus on all of the three features and put the role of the calendar time on center stage rather than the tick time.

In this paper we develop a novel continuous calendar time framework for prices out of a desire to capture these features in an analytically tractable but potentially semi-parametric manner. We

will show that our model captures the serial dependence in price changes over three different time scales: 0.1 seconds, 1 seconds, 10 seconds and 1 minute.

Although our work is a distinctive move away from the existing literature, it will relate to a number of aspects that are often dealt with one at a time. Here we discuss some of this material.

Most of the econometric work on the modelling of high frequency financial data focuses on the times between trades and quote updates. This literature splits into two: the modelling of the conditional mean duration between events given past data and the modelling of the conditional intensity of trade arrivals given past data. It is reviewed by, for example, Engle (2000), Russell and Engle (2010) and Hautsch (2012). The former was initiated in Engle and Russell (1998) and contributions include Zhang, Russell, and Tsay (2001), Hamilton and Jordá (2002) and Cipollini, Engle, and Gallo (2009). The latter focuses around, for example, Russell (1999), Bowsher (2007) and Hautsch (2012), building on the stochastic analysis of Hawkes (1972).

There is much less econometric work on the discreteness of high frequency data. Papers that focus on discreteness include Rydberg and Shephard (2003), Russell and Engle (2006), Liesenfeld, Nolte, and Pohmeier (2006), Large (2011), Oomen (2005), Oomen (2006) and Griffin and Oomen (2008). Some of the early work on the impact of discreteness in practice includes Harris (1990), Gottlieb and Kalay (1985), Ball, Torous, and Tschoegl (1985) and Ball (1988). A significant approach to deal with discreteness is to build continuous time models for prices on the positive half-line that are then rounded to induce discreteness, sometimes with extra additive measurement error. Examples include, for a variety of purposes, Hasbrouck (1999), Rosenbaum (2009), Delattre and Jacod (1997), Jacod (1996) and Li and Mykland (2014). Also note the statistical work by Kolassa and McCullagh (1990).

The most comparable literatures to our own include Bacry, Delattre, Hoffman, and Muzy (2013a), Bacry, Delattre, Hoffman, and Muzy (2013b), Fodra and Pham (2013a) and Fodra and Pham (2013b). See also Fauth and Tudor (2012). Bacry et al. model the evolution of price changes as the difference of two self-exciting and interacting simple counting processes. These multivariate Hawkes processes have intensities that react to previous moves, so an up move in the price will temporarily increase the intensity of a down move, creating the chance that the move will turn out to be fleeting. This elegant model only allows unit price moves, but could be extended, while the dynamics is tightly parameterized. Fodra and Pham directly assume an irreducible Markov chain structure on the sequence of price changes, which is less flexible as only the current price direction will impact the next jump direction.

Our paper has its intellectual roots in two papers. Barndorff-Nielsen, Pollard, and Shephard (2012) build Lévy processes (continuous time random walks) that are integer-valued. We are also inspired by the stationary integer-valued processes of Barndorff-Nielsen, Lunde, Shephard, and Veraart (2014). Their processes are related to the up-stairs processes of Wolpert and Taqqu (2005) and the random measure processes of Wolpert and Brown (2011). Both of these processes are stationary. Barndorff-Nielsen, Lunde, Shephard, and Veraart (2014) also bring out the relationship between their processes and  $M/G/\infty$  queues (e.g. Lindley (1956), Reynolds (1968) and Bartlett (1978, Ch. 6.31)). They also connect these models to the so-called mixed moving average models of Surgailis, Rosinski, Mandrekar, and Cambanis (1993). See also the work of Fuchs and Stelzer (2013). None of these papers can be used directly as a coherent model of high frequency data. Our paper fills this essential gap.

Our new approach will involve events arriving in continuous time, whose impacts on the prices may be fleeting and of variable size. The model is directly formulated in terms of the price impact of news. Each fleeting move is a temporary change in the price that has a random survival time until its impact disappears. The model allows a decomposition of the discrete price process into a continuous time random walk (due to permanent impacts) plus a temporary fleeting component (due to market microstructure noise). The resulting càdlàg price process will be a piecewise constant semimartingale with finite activity, finite variation and no Brownian motion component. It is also capable of generating negative autocorrelations for price changes that is consistent with the empirical observations. We have non-parametric freedom in choosing the level of dependence in the noises—which can even have long memory if this is needed in the data. Alternatively, the applied researcher can tightly parameterize the model if necessary.

In this paper our model is static: the parameters are time-invariant, not adapting to past data. This is an important deficiency, but a stochastic time-change can deal with most of these challenges. We will address them in a follow up paper. Our goal here is to set down a framework that is both empirically compelling and statistically scalable in the future work.

Finally, throughout our empirical work we have used trade prices. We could have used our model on the best bid or ask prices. This would have had the advantage that the best bid or ask are prices an investor can trade immediately, while trade prices are those which have been traded by someone in the past.

The outline of this paper is as follows. In Section 2 we set up the probability structure of our model and review a couple of building blocks from previous papers. In Section 3 we introduce the

core of our contribution: defining our model for prices and providing an analysis of this process and the corresponding return sequence. In Section 4 we discuss the moment-based estimations for these models, while in Section 5 we apply these estimation methods to real data. Section 6 concludes. The Appendix has four sections. The first collects the proofs of the various theorems given in the main text of the paper as well as the details of some remarks. The second outlines how to compute probability mass functions of price changes using the inverse fast Fourier transform. The third details our data cleaning procedures. The fourth gives a non-parametric estimator of a part of our model.

## 2 Integer-valued stochastic process in continuous time

### 2.1 Poisson random measure

Our framework will revolve around (i) events arriving in continuous time, (ii) events whose impacts may be fleeting with a random survival time and (iii) events of variable size and direction. To generate these events, it is natural to base the underlying randomness on a three dimensional Poisson random measure  $N$  (see, e.g., Kingman (1993) for a review) with intensity measure

$$\mathbb{E}(N(dy, dx, ds)) = \nu(dy)dxds.$$

Here  $s$  is time (with arrivals randomly scattered on  $\mathbb{R}$ ),  $x$  is random height (uniformly scattered over  $[0, 1]$ ), which will be the random source for the survival time of the fleeting event, and  $y$  marks integer size (with direction) of events. These names will become clearer later in Figure 1 and 2. As with all Poisson random measures, the chance that there are two points with common height or time is zero.

Price moves can be up or down, but zero is ruled out. Thus the size of the events will be assumed to have a Lévy measure  $\nu(dy)$  concentrated on  $y \in \mathbb{Z} \setminus \{0\}$ , the non-zero integers. With no confusions, we will sometimes abuse the notation  $\nu(y)$  to denote the mass of the Lévy measure centered at  $y$ , so

$$\nu(dy) = \sum_{y \in \mathbb{Z} \setminus \{0\}} \nu(y) \delta_{\{y\}}(dy),$$

where  $\delta_{\{y\}}(dy)$  is the Dirac point mass measure centered at  $y$ . Throughout this paper, we assume that<sup>1</sup>  $\|\nu\| \triangleq \int_{-\infty}^{\infty} \nu(dy) = \sum_{y \in \mathbb{Z} \setminus \{0\}} \nu(y) < \infty$ .

---

<sup>1</sup>An equal sign with a triangle above  $\triangleq$  means a definition.

**Remark 1** We will see in a moment that the mass  $\nu(y)$  represents the intensity of events of size  $y$ , so in aggregate the Lévy measure  $\nu$  will simultaneously controls the scope of all the possible jumping sizes in addition to their individual intensity.  $\diamond$

## 2.2 Lévy basis and Lévy process

Our model will be based on the resulting homogeneous<sup>2</sup> Lévy basis on  $[0, 1] \times \mathbb{R} \mapsto \mathbb{Z} \setminus \{0\}$ , which records the size  $y \in \mathbb{Z} \setminus \{0\}$  at each point in time  $s \in \mathbb{R}$  and height  $x \in [0, 1]$ . It is given by

$$L(dx, ds) \triangleq \int_{-\infty}^{\infty} y N(dy, dx, ds), \quad (x, s) \in [0, 1] \times \mathbb{R},$$

and for any Borel measurable set  $S \subseteq [0, 1] \times \mathbb{R}$  we let

$$L(S) \triangleq \int_{[0,1] \times \mathbb{R}} 1_S(x, s) L(dx, ds),$$

where  $1_S$  is the indicator function of  $S$ . To connect with the later discussion, a Lévy process generated from  $L$  can be defined as

$$L_t \triangleq L(D_t) = \int_0^t \int_0^1 L(dx, ds),$$

where  $D_t \triangleq [0, 1] \times (0, t]$  is a rectangle that grows with  $t$ , so  $L_t$  just counts up the points in the Lévy basis from time 0 to time  $t$ .

**Example 1** Suppose that  $\nu(dy) = \|\nu\| (0.5 \times \delta_{\{1\}}(dy) + 0.5 \times \delta_{\{-1\}}(dy))$ . Then  $\|\nu\|$  is the arrival rate of events in time, each with a random height and having size  $\pm 1$  with equal probability. Figure 1 plots a Skellam Lévy basis  $L$  using  $\|\nu\| = 7$ , taking on 1,  $-1$  with black and white dots respectively. The lower panel shows the corresponding Skellam Lévy process, which is the difference of two independent Poisson processes with intensity  $\|\nu\|/2$ .  $\diamond$

## 2.3 Stationary trawl process

To introduce fleeting moves, the random heights in the Lévy basis will be exploited. We start from a fixed shape<sup>3</sup>  $A \subseteq [b, 1] \times (-\infty, 0]$ , where  $b \in [0, 1]$  is called the permanence parameter. Throughout we assume that the area of  $A$ ,  $leb(A)$ , is finite. Barndorff-Nielsen, Lunde, Shephard, and Veraart (2014) call  $A$  a trawl for the case of  $b = 0$ , which is the core of their stationary integer-valued processes. Here we call  $A$  a squashed trawl, a minor variant on their idea.

<sup>2</sup>Homogeneity here refers to the height and time as the points in the Lévy basis are uniformly scattered on  $[0, 1] \times \mathbb{R}$ .

<sup>3</sup>For technical reasons, we need to assume that the fixed set  $A$  is *closed on the right* and *open on the left*, that is, for every  $x \in [b, 1]$ , all the set  $A \cap \{(x, s) : s \leq 0\}$  must be a union of half-closed intervals of the form  $(a, b]$ . This is enforced so the resulting jump process is *càdlàg*. Besides, we need to assume that the projection of  $A$  on the vertical axis has Lebesgue measure  $b$  so the parameter  $b$  is well-defined and statistically identifiable.

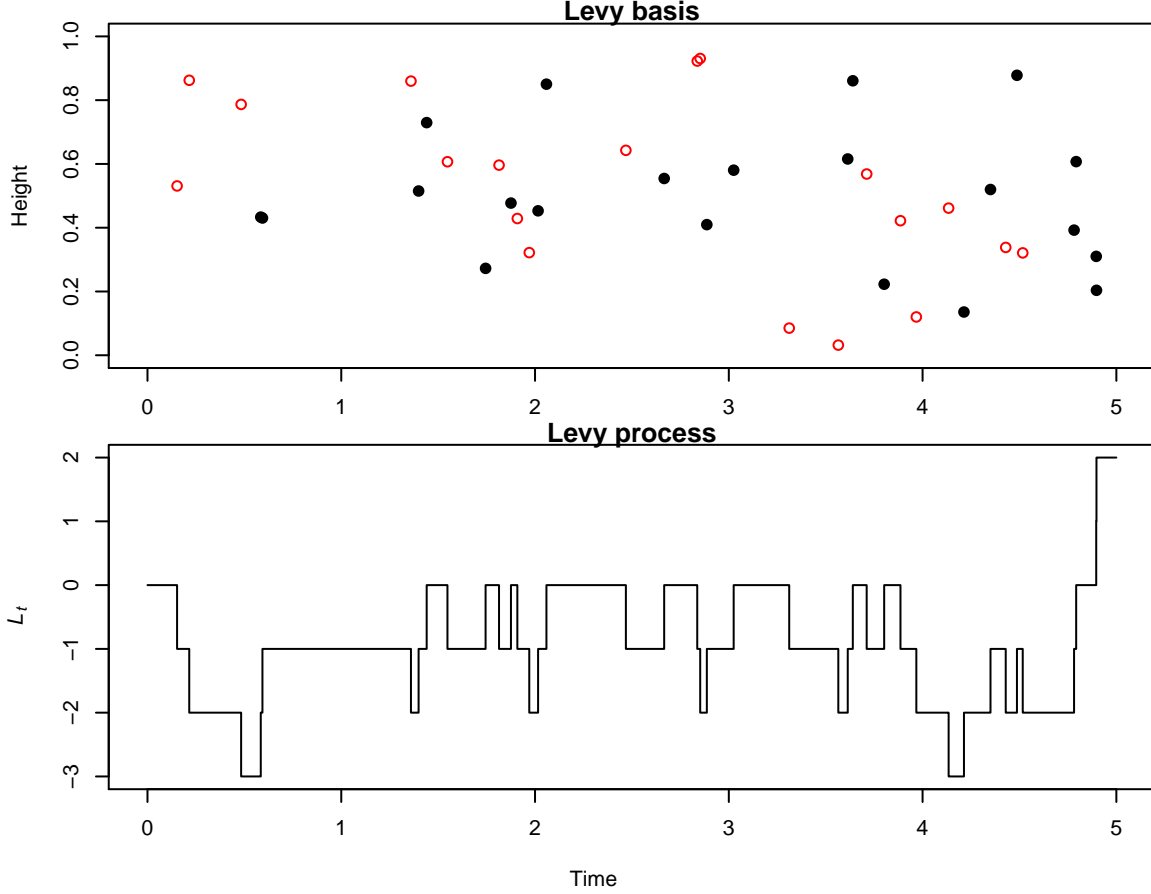


Figure 1: Top: Lévy basis  $L(dx, ds)$ , where the horizontal axis  $s$  is time and the vertical axis  $x$  is height, which plays no role in this construction of the Lévy process in the lower panel. Black dots denote 1, white ones  $-1$ . Bottom: The corresponding Lévy process, which sums up all the effects in the Lévy basis (in the upper panel) from time 0 to time  $t$ , while the vertical axis here is the value of the Lévy process, which jumps up by 1 by the effect of black dots and down by 1 by white ones. Code: `LpTprocess_Illustration.R`.

**Definition 1** A squashed trawl  $A$  defined by a trawl function  $d$  is obtained from

$$A \triangleq \{(x, s) : s \leq 0, b \leq x < d(s)\},$$

where  $d : (-\infty, 0] \mapsto [b, 1]$  is continuous and monotonically increasing ( $d(s_1) \leq d(s_2)$  for all  $s_1 \leq s_2 \leq 0$ ) and satisfies the following regularity conditions:  $d(-\infty) \triangleq \lim_{s \rightarrow -\infty} d(s) = b$ ,  $d(0) = 1$  and  $\int_{-\infty}^0 (d(s) - b) ds < \infty$ .  $\diamond$

We now drag the set  $A$  through time without changing its height

$$A_t \triangleq A + (0, t) = \{(x, s) : s \leq t, b \leq x < d(s - t)\}, \quad t \geq 0.$$

Notice that  $leb(A_t) = leb(A) < \infty$  for all  $t \geq 0$ . Then the *stationary (trawl) process* is defined as  $L(A_t)$  for  $t \geq 0$ . In a moment this will be a component of our proposed price process.

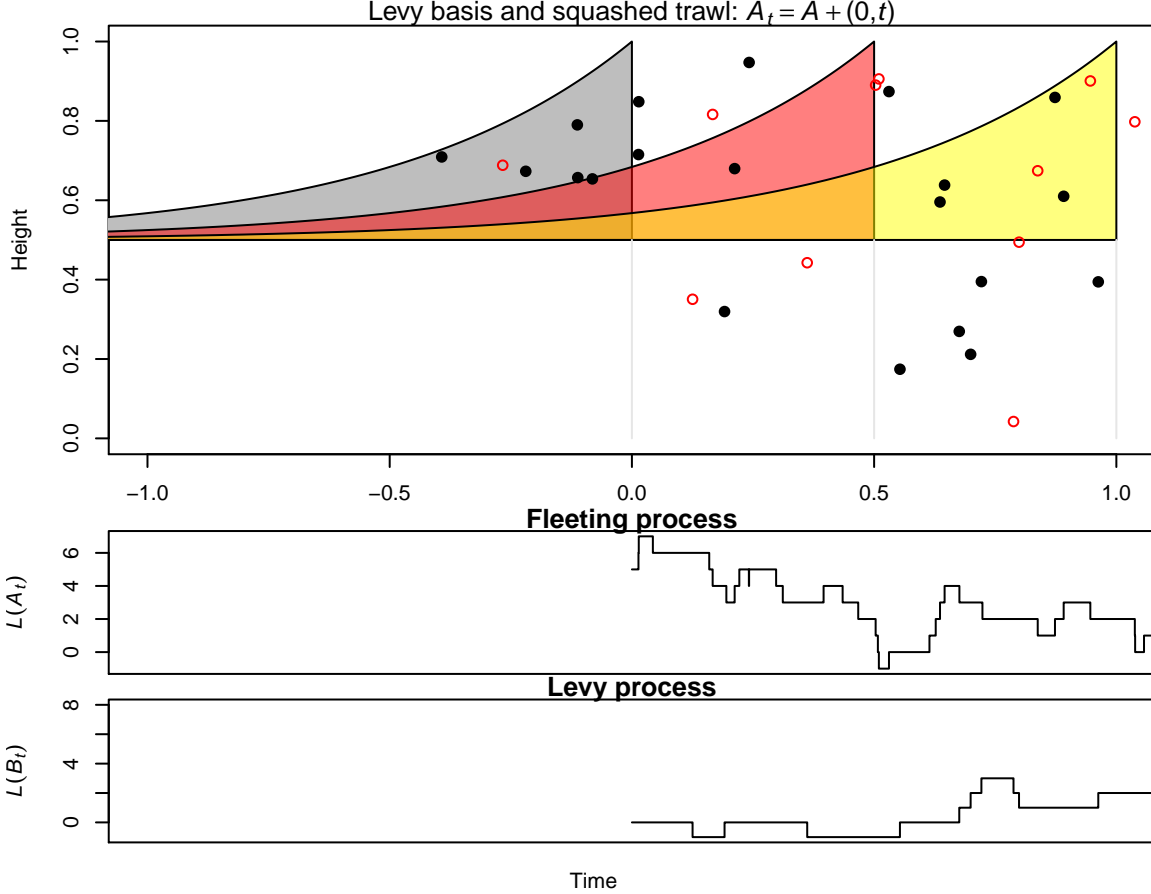


Figure 2: A moving squashed trawl  $A_t$  is joined by the Lévy basis  $L(dx, ds)$ , where the horizontal axis  $s$  is time and the vertical axis  $x$  is height. The shaded area is an example of the trawl  $A$  generated by the trawl function  $d$ , while we also show the outlines of  $A_t$  when  $t = 1/2$  and  $t = 1$ . Also shown below is the implied stationary process  $L(A_t)$  and the Lévy process  $L(B_t)$  for  $t \geq 0$ , where  $B_t = [0, b) \times (0, t]$ . Code: `LpTprocess_Illustration.R`.

**Example 2** The upper panel of Figure 2 illustrates  $A_t$  when  $d(s) = 0.5 + (1 - 0.5)e^{2s}$ . The middle panel of Figure 2 also shows  $L(A_t)$  when  $L$  is a Skellam basis, which sums up all the effects (both positive and negative) captured by (or surviving in) the trawl. Dynamically,  $L(A_t)$  will move up by 1 if the moving squashed trawl  $A_t$  either captures one positive event that has height above  $b$  or releases a negative one; conversely, it will move down by 1 if vice versa. Also notice that  $L(A_0)$  might not be necessarily zero.  $\diamond$

Throughout we use  $\kappa_j(X)$  as a generic notation for the  $j$ -th cumulant of an arbitrary random variable  $X$ . Recall that  $L_1 = L(D_1) = \int_0^1 \int_0^1 L(dx, ds)$ . In the following Proposition, we rephrase the key properties of the stationary process  $L(A_t)$  mentioned in Barndorff-Nielsen, Lunde, Shephard, and Veraart (2014) under the squashed trawl variant.

**Proposition 1** *If  $\text{leb}(A) < \infty$ , then  $L(A_t)$  is well-defined and strictly stationary. If  $\kappa_2(L_1) < \infty$  as well, then it is covariance stationary and for  $t > s$*

$$\text{Cov}(L(A_t), L(A_s)) = \text{leb}(A_{t-s} \cap A) \kappa_2(L_1), \quad \text{Cor}(L(A_t), L(A_s)) = \frac{\text{leb}(A_{t-s} \cap A)}{\text{leb}(A)}.$$

Furthermore, for any  $t \geq 0$ ,

$$\text{leb}(A_t \cap A) = \int_{-\infty}^{-t} (d(s) - b) \, ds \tag{1}$$

is monotonically decreasing as  $t$  increases.

### 3 Integer-valued price process with fleeting moves

#### 3.1 Definition

We now turn to the main contribution of this paper. Our proposed integer-valued price process is defined as

$$P_t \triangleq V_0 + L(C_t) = V_0 + L(A_t) + L(B_t), \quad t \geq 0,$$

where we recall that  $A_t = A + (0, t)$  and

$$B_t \triangleq [0, b) \times (0, t], \quad C_t \triangleq A_t \cup B_t.$$

Here  $V_0$  is a non-negative integer;  $L$  is a Lévy basis;  $L(A_t)$  is a stationary integer-valued process that controls the fleeting movements of the price;  $V_0 + L(B_t)$  is an integer-valued Lévy process (initiating at  $V_0$ , which is aggregated from the permanent arrivals in the past) that represents a non-stationary component of the price process. Recall that  $L(B_t) = \int_0^t \int_0^b L(dx, ds)$ ,  $t \geq 0$ .

**Example 3 (Continued from Example 2)** The lower panel of Figure 2 shows the corresponding Skellam Lévy process  $L(B_t)$ . Notice that there are no permanent events in the negative time because they have been taken into account in  $V_0$ . Over short time scales it is hard to tell the difference between these two processes  $L(A_t)$  and  $L(B_t)$ , but over long time scales they are starkly different. For any event arrival, if the random height  $x$ —not size  $y$ —is above  $b$ , then this effect stays in  $A_t$  temporarily and hence is fleeting; if the height is below  $b$ , then this effect is always in  $B_t$  and hence permanent.  $\diamond$

This càdlàg price process has finite activity (i.e. finite number of jumps in any finite interval of time, due to the Lévy basis being of finite activity), is piecewise-constant (i.e. jumps only when there are arrivals or departures) and consequently has finite variation. Thus the model is in keeping with the empirical data.



**Remark 2** The integer-valued price process  $P_t$  is a semimartingale with respect to its natural filtration. The details can be found in Appendix A. Here we especially point out that a semimartingale model that allows the fleeting behavior is atypical in the literature of market microstructure.  $\diamond$

**Remark 3** In this model some price moves have permanent impact. Others are fleeting, being reversed rapidly. The lifetime of an arrival event is determined by the trawl function. Assume that the trawl function  $d$  is strictly increasing and hence invertible. Then we can think of  $G(s) \triangleq 1 - d(-s)$  (with  $G(\infty) \triangleq 1$ ) as the cumulative distribution function of the lifetime for  $s \geq 0$ . Thus, for  $U \sim U(0, 1)$ , the standard uniform distribution,  $G^{-1}(U)$  means the lifetime of an arrival event with random height  $U$ . When  $U \leq b$ , then  $G^{-1}(U) = \infty$ , meaning it is permanent. For  $U > b$  then the event will last  $G^{-1}(U) < \infty$ , meaning it is fleeting.  $\diamond$

**Remark 4** If a new piece of news arrives at time  $t$ , it impacts the price through the arrival of a new point in the Lévy basis. For concreteness of exposition here, suppose it has unit impact. Then the expected impact of this individual event at time  $t + s$  is  $d(-s)$ , where  $s \geq 0$ . Hence the trawl function directly describes the *price impact curve* of news arrivals. It is tempting to label  $d$  the price impact function, but we continue with the trawl nomenclature. The permanent impact of the unit news is thus  $b$ .  $\diamond$

### 3.2 Distribution of price changes

The following Theorem characterizes the distribution of price changes over a time length  $t$ .

**Theorem 1** *Let  $A \setminus B$  be set subtraction (all elements of  $A$  except those that are also in  $B$ ). Then*

$$P_t - P_0 = L(C_t) - L(C_0) = L(C_t \setminus C_0) - L(C_0 \setminus C_t),$$

where  $L(C_t \setminus C_0)$  is independent of  $L(C_0 \setminus C_t)$ . Consequently the logarithmic characteristic function of returns is

$$\begin{aligned} C(\theta \ddagger P_t - P_0) &= btC(\theta \ddagger L_1) + leb(A_t \setminus A)(C(\theta \ddagger L_1) + C(-\theta \ddagger L_1)), \quad \text{where} \\ C(\theta \ddagger L_1) &\triangleq \log \mathbb{E} \left( e^{i\theta L_1} \right), \quad i \triangleq \sqrt{-1}, \quad L_1 = \int_0^1 \int_0^1 L(dx, ds). \end{aligned}$$

Furthermore, if the  $j$ -th cumulant of  $L_1$  exists, then

$$\begin{aligned} \kappa_j(P_t - P_0) &= bt\kappa_j(L_1), \quad j = 1, 3, 5, \dots, \\ \kappa_j(P_t - P_0) &= (bt + 2leb(A_t \setminus A))\kappa_j(L_1), \quad j = 2, 4, 6, \dots \end{aligned}$$

**Remark 5** Notice that  $C_t \setminus C_0$  has the physical interpretation of arrivals during the time period 0 to  $t$  for both positive and negative effects;  $C_0 \setminus C_t$  are departures instead. Further, the equalities

$$leb(A_t \setminus A) = leb(A) - leb(A_t \cap A) = leb(A \setminus A_t) = \int_{-t}^0 (d(s) - b) ds \quad (2)$$

are often helpful in calculations.  $\diamond$

**Remark 6** The probability mass function of  $P_t - P_0$  can be computed using the characteristic function and the inverse fast Fourier transform. The details can be found in the Appendix B.  $\diamond$

**Remark 7** Even though our model is written down for the study of high frequency data, it can easily connect back to those diffusion based models that are commonly used to study data at less high frequency. Theorem 1 further implies that the fleeting price process becomes a Brownian motion at lower frequency. Precisely, if  $\kappa_2(L_1) < \infty$  and  $X_t^{(c)} \triangleq c^{-1/2} (P_{ct} - P_0 - bct\kappa_1(L_1))$ , then  $X^{(c)} \xrightarrow{\mathcal{L}} W$  as  $c \rightarrow \infty$ , where  $W$  is a Wiener process or a standard Brownian motion.  $\diamond$

Let  $\Delta P_t \triangleq P_t - P_{t-}$  be the instantaneous jump (or return) of the price process at time  $t$ . By the instantaneous jumping distribution, we mean the probability of  $\Delta P_t = y$  given that  $\Delta P_t \neq 0$  for  $y \in \mathbb{Z} \setminus \{0\}$ . In the following we give a closed-form expression for this distribution.

**Theorem 2** *The instantaneous jumping distribution is*

$$\mathbb{P}(\Delta P_t = y | \Delta P_t \neq 0) = \frac{\nu(y) + \nu(-y)(1-b)}{(2-b)\|\nu\|}. \quad (3)$$

Notice that the trawl function  $d$  in the fleeting component has no impact on the instantaneous jumping distribution: what is important is  $b$ , which controls the amount of potential departures among all the arrival jumps. Besides, the left-hand side of equation (3) can be easily estimated from the data, so we might in turn estimate  $\nu$  and  $b$  by simple moment-matching. To calibrate the trawl, Theorem 1 imply the easy use of sample cumulants across different  $t$  to infer the shape of  $leb(A_t \setminus A)$  and hence  $d$ . We will see these in Section 4 later.

### 3.3 Autocorrelation structure of price changes

Theorem 3 captures the linear dependence in the price changes.

**Theorem 3** *Assume that  $\kappa_2(L_1) < \infty$ . Then the price changes have the autocorrelation structure, for some sampling interval  $\delta > 0$  and  $k = 1, 2, \dots$*

$$\gamma_k \triangleq \text{Cov}((P_{(k+1)\delta} - P_{k\delta}), (P_\delta - P_0))$$

$$\begin{aligned}
&= (\text{leb}(A_{(k+1)\delta}\setminus A) - 2\text{leb}(A_{k\delta}\setminus A) + \text{leb}(A_{(k-1)\delta}\setminus A)) \kappa_2(L_1), \\
\rho_k &\triangleq \text{Cor}((P_{(k+1)\delta} - P_{k\delta}), (P_\delta - P_0)) \\
&= \frac{\text{leb}(A_{(k+1)\delta}\setminus A) - 2\text{leb}(A_{k\delta}\setminus A) + \text{leb}(A_{(k-1)\delta}\setminus A)}{b\delta + 2\text{leb}(A_\delta\setminus A)}.
\end{aligned}$$

**Corollary 1**  $\rho_k \leq 0$  for all  $k = 1, 2, \dots$ . This inequality becomes strict when  $d$  is strictly increasing (i.e.  $d(s_1) < d(s_2)$  for all  $s_1 < s_2 \leq 0$ ).

**Remark 8** For a pure Lévy process ( $b = 1$ ),  $\text{leb}(A_t\setminus A) = 0$  for all  $t$ , so clearly  $\rho_k = 0$  for all  $k = 1, 2, \dots$ , as expected. On the other hand, equation (2) implies

$$\lim_{\delta \rightarrow 0} \frac{\text{leb}(A_{l\delta}\setminus A)}{\delta} = (1-b)l, \quad \lim_{\delta \rightarrow \infty} \text{leb}(A_{l\delta}\setminus A) = \text{leb}(A), \quad l = 1, 2, \dots,$$

so it is easy to see that, for any fixed  $k = 1, 2, \dots$ ,

$$\lim_{\delta \rightarrow 0} \rho_k = \lim_{\delta \rightarrow \infty} \rho_k = 0.$$

Thus, Corollary 1 implies that  $\rho_k$  is not a monotonic function of the sampling interval  $\delta$ . This matches with the empirical data, which we will see later in Figure 7.  $\diamond$

### 3.4 Power variation

Quadratic variation plays a central role in stochastic analysis and modern finance (e.g. Andersen, Bollerslev, Diebold, and Labys (2001) and Barndorff-Nielsen and Shephard (2002)). For any  $r \geq 0$ , we define the  $r$ -th power Lévy basis as

$$\Sigma(dx, ds; r) \triangleq \int_{-\infty}^{\infty} |y|^r N(dy, dx, ds)$$

with mean measure

$$\mu(dx, ds; r) \triangleq dx ds \int_{-\infty}^{\infty} |y|^r \nu(dy),$$

assuming that  $\int_{-\infty}^{\infty} |y|^r \nu(dy) < \infty$ . Theorem 4 relates  $\Sigma$  to

$$\{P\}_t^{[r]} = \lim_{\delta \rightarrow 0} \sum_{k=1}^{t/\delta} |P_{k\delta} - P_{(k-1)\delta}|^r = \sum_{0 < s \leq t} |\Delta P_s|^r,$$

the  $r$ -th (unnormalized) power variation, which was formalized in finance by Barndorff-Nielsen and Shephard (2004). The special case of  $r = 2$  yields the quadratic variation. Notice that in our model we can compute  $\{P\}_t^{[r]}$  exactly, just using the price path. It is finite for all  $r \geq 0$  with probability one. This contrasts with the vast majority of work in econometrics that would take  $\{P\}_t^{[r]}$  as infinity due to the impact of market microstructure.

**Theorem 4** For any  $r \geq 0$ , the  $r$ -th power variation is

$$\begin{aligned} \{P\}_t^{[r]} &= \Sigma(B_t; r) + Z_t^{[r]}, \quad B_t \triangleq [0, b] \times (0, t], \\ Z_t^{[r]} &\triangleq \Sigma(H_t; r) + \Sigma(G_t; r), \quad H_t \triangleq [b, 1] \times (0, t], \quad G_t \triangleq (H_t \cup A) \setminus A_t. \end{aligned}$$

Furthermore, their expectations are

$$\mathbb{E} \left( \{P\}_t^{[r]} \right) = (2 - b) t \int_{-\infty}^{\infty} |y|^r \nu(dy). \quad (4)$$

**Remark 9** Like (3), (4) does not feature the trawl function, as each arrival is joined by a departure. Hence it is always robust to the details of  $d$ . Further,

$$\mathbb{E} \left( \{P\}_t^{[r]} \right) = \mathbb{E} \left( \{P\}_t^{[0]} \right) \int_{-\infty}^{\infty} |y|^r \frac{\nu(dy)}{\|\nu\|}.$$

Notice that  $\{P\}_t^{[0]}$  counts the total number of jumps of the process  $P$  up to time  $t$ , so throughout we call it the counting process of price moves. It will also play an important role in Section 4 for the construction of our moment-based estimate for the model parameters.  $\diamond$

We think of the random  $Z_t^{[r]}$ , which is finite with probability one, as the component of power variation due to fleeting moves in prices, for

$$\{P\}_t^{[r]} - \{L(B_t)\}_t^{[r]} = Z_t^{[r]}$$

is the asymptotic stochastic bias of the power variation.

High frequency econometricians would typically think of terms like  $Z_t^{[2]}$  as the driver of the bias in realized variance due to market microstructure effects (e.g. Hansen and Lunde (2006), Zhang (2006), Jacod, Li, Mykland, Podolskij, and Vetter (2009), Mykland and Zhang (2012) and Barndorff-Nielsen, Hansen, Lunde, and Shephard (2008)), but it is typically infinite in their studies while here and empirically it is finite with probability one<sup>4</sup>.

We recall from Theorem 1 that

$$\mathbb{E}(P_t - P_0) = bt\kappa_1(L_1), \quad \text{Var}(P_t - P_0) = \{bt + 2leb(A_t \setminus A)\} \kappa_2(L_1).$$

---

<sup>4</sup>Econometricians use a variety of models for market microstructure noise. Typically the noise appears each time a trade happens, e.g. in Zhou (1996) the noises are i.i.d. with a zero mean. Hence we can think of these types of models as purely statistical measurement error models. In more recent times, the i.i.d. assumption has been generalized to allow some levels of temporal dependence and volatility clustering, but all in tick time instead of the calendar time. All of these models of noise have the power variations being infinity. There is another set of papers that think of prices as being a rounded version of a semimartingale. This is closer to our paper, but here the level of dependence in price moves is entirely dependent on the size of the ticks in comparison to the volatility of the semimartingale. This is insufficiently flexible to fit the data. Another set of papers round a semimartingale with additive measurement noise, but again this has infinite power variation, which does not coincide with the empirical observations.

We now think about returns over the time interval  $[0, T]$ , so the realized variance is

$$RV^{(n)} \triangleq \sum_{k=1}^n (P_{k\delta_n} - P_{(k-1)\delta_n})^2, \quad \delta_n \triangleq \frac{T}{n}.$$

**Proposition 2** *Assume that  $\kappa_2(L_1) < \infty$ . Then*

$$\mathbb{E} \left( RV^{(n)} \right) = \left( b + 2 \frac{leb(A_{\delta_n} \setminus A)}{\delta_n} \right) T \kappa_2(L_1) + b^2 T \delta_n \kappa_1^2(L_1).$$

We can set the context of Proposition 2 by discussing the two extremes  $n = 1$  and  $n \rightarrow \infty$  for a large  $T$ . For  $n = 1$ , as  $T \rightarrow \infty$ ,

$$\begin{aligned} \mathbb{E} \left( RV^{(1)} \right) &= \left( b + 2 \frac{leb(A_T \setminus A)}{T} \right) T \kappa_2(L_1) + b^2 T^2 \kappa_1^2(L_1) \\ &\approx bT \kappa_2(L_1) + b^2 T^2 \kappa_1^2(L_1) \\ &= \kappa_2(L(B_T)) + (\kappa_1(L(B_T)))^2 = \mathbb{E} \left( L(B_T)^2 \right), \end{aligned}$$

where the second line uses  $leb(A_T \setminus A) \approx leb(A)$ . For  $n \rightarrow \infty$  and a fixed  $T$ ,

$$\lim_{n \rightarrow \infty} \mathbb{E} \left( RV^{(n)} \right) = (2 - b) T \kappa_2(L_1).$$

Therefore, in this model the realized variance and the volatility of price changes are highly distorted by the fleeting component. A variance signature plot ( $RV^{(T/\delta)}$  against  $\delta$ ) for our model will start out high around  $(2 - b) T \kappa_2(L_1)$  (the expected quadratic variation of the price process) for large  $n$  (dense sampling) and tend downwards to approximately  $bT \kappa_2(L_1)$  (the expected quadratic variation of the Lévy process component, assuming that  $\kappa_1(L_1)$  being very small). A minor variant of this type of plots, which we will discuss in Remark 12, can be found in Figure 8 later in our empirical work.

### 3.5 Generalized compound representation

As the price process is of finite activity, it can be usefully written as a generalized compound process, driven by the counting process of price moves. Here we detail this. First recall that  $G(s) = 1 - d(-s)$  (with  $G(\infty) = 1$ ) denotes the cumulative distribution function of the lifetime for  $s \geq 0$ .

$L(A_0)$  is built out of  $N^{A^*}$  initial surviving events, who arrive at times  $\tau_1^{A^*} < \dots < \tau_{N^{A^*}}^{A^*} \leq 0$  and jump with sizes  $\varkappa_1^{A^*}, \dots, \varkappa_{N^{A^*}}^{A^*}$ . Each arrival has a lifetime  $G^{-1}(U_1^{A^*}), \dots, G^{-1}(U_{N^{A^*}}^{A^*})$ , where  $\tau_j^{A^*} + G^{-1}(U_j^{A^*}) > 0$  and  $U_j^{A^*} \stackrel{\text{i.i.d.}}{\sim} U(b, 1)$ . Thus we can write  $L(A_0) = \sum_{j=1}^{N^{A^*}} \varkappa_j^{A^*} 1_{\tau_j^{A^*} + G^{-1}(U_j^{A^*}) > 0}$ . When  $\varkappa_j^{A^*} = 1$  for all  $j$ , this representation has a close connection to a  $M/G/\infty$  queue (i.e. Markov arrivals, with a fixed service time distribution  $G$ , but with an infinite number of servers).

As time progresses some events die and the initial values thin down to  $\sum_{j=1}^{N_t^{A^*}} \varkappa_j^{A^*} 1_{\tau_j^{A^*} + G^{-1}(U_j^{A^*}) > t}$  while new ones are born  $\sum_{j=1}^{N_t^A} \varkappa_j^A 1_{\tau_j^A + G^{-1}(U_j^A) > t}$ , where  $N_t^A$  is the number of births from time 0 to time  $t$  with heights greater than  $b$ . The corresponding  $\tau_j^A$ 's and  $\varkappa_j^A$ 's are the arrival times of these events and size of the moves. Thus the stationary process is

$$L(A_t) = \sum_{j=1}^{N_t^{A^*}} \varkappa_j^{A^*} 1_{\tau_j^{A^*} + G^{-1}(U_j^{A^*}) > t} + \sum_{j=1}^{N_t^A} \varkappa_j^A 1_{\tau_j^A + G^{-1}(U_j^A) > t}, \quad t \geq 0.$$

The corresponding impact of the permanent changes is a compound Poisson process  $L(B_t) = \sum_{j=1}^{N_t^B} \varkappa_j^B$ , where  $N_t^B$  counts the number of permanent arrivals up to time  $t$  and  $\tau_j^B$ 's and  $\varkappa_j^B$ 's are the corresponding arrival times and jump sizes. We also write  $\tau_k$  to be any one of the jumping times from resulted chronologically from both the arrivals and departures; similarly for  $\varkappa_k$ . Then  $N_t \triangleq \#\{k : \tau_k \leq t\}$  counts the total number of jumps of the price process up to time  $t$ .

All these imply that

$$P_t = V_0 + \sum_{j=1}^{N_t^{A^*}} \varkappa_j^{A^*} 1_{\tau_j^{A^*} + G^{-1}(U_j^{A^*}) > t} + \sum_{j=1}^{N_t^A} \varkappa_j^A 1_{\tau_j^A + G^{-1}(U_j^A) > t} + \sum_{j=1}^{N_t^B} \varkappa_j^B = P_0 + \sum_{k=1}^{N_t} \varkappa_k. \quad (5)$$

Equation (5) is called a generalized compound representation. It links with the very large literature on the use of compound Poisson processes in financial econometrics, e.g. Press (1967). However, here we allow a fraction of the jumps to be fleeting, so the resulting counting process  $N_t$  is not simply a Poisson process.

### 3.6 Parameterized trawl function

To fit this type of model using data, it is sometimes helpful to index the trawl function by a small number of parameters. Throughout we work within the following framework.

**Definition 2** A superposition trawl function has

$$d(s) = b + (1 - b) \int_0^\infty e^{\lambda s} \pi(d\lambda), \quad s \leq 0, \quad (6)$$

where  $\pi$  is an arbitrary probability measure on  $(0, \infty)$ . We constrain the superposition class to where  $\int_0^\infty \lambda^{-1} \pi(d\lambda) < \infty$ .  $\diamond$

Whatever the probability measure  $\pi$  the resulting  $d$  always exists since  $0 \leq \int_0^\infty e^{\lambda s} \pi(d\lambda) \leq \int_0^\infty \pi(d\lambda) = 1$ , as  $s \leq 0$ . The constraint  $\int_0^\infty \lambda^{-1} \pi(d\lambda) < \infty$  is needed to ensure that the area of  $A$  is finite, for this area is

$$leb(A) = \int_{-\infty}^0 \int_b^{d(s)} dx ds = \int_{-\infty}^0 (d(s) - b) ds = (1 - b) \int_{-\infty}^0 \int_0^\infty e^{\lambda s} \pi(d\lambda) ds$$

$$= (1-b) \int_0^\infty \int_{-\infty}^0 e^{\lambda s} ds \pi(d\lambda) = (1-b) \int_0^\infty \frac{1}{\lambda} \pi(d\lambda). \quad (7)$$

Using equation (1) the superposition framework (6) has

$$leb(A_t \cap A) = (1-b) \int_0^\infty \frac{e^{-t\lambda}}{\lambda} \pi(d\lambda), \quad t \geq 0,$$

so, combining it with equation (7), we have

$$\int_0^\infty \text{Cor}(L(A_t), L(A_0)) dt = \frac{\int_0^\infty \lambda^{-2} \pi(d\lambda)}{\int_0^\infty \lambda^{-1} \pi(d\lambda)}.$$

Thus, the superposition trawl has long memory if and only if  $\int_0^\infty \lambda^{-2} \pi(d\lambda) = \infty$ .

In the following we focus only on choices of specific  $\pi$ . These special cases have been analyzed in Barndorff-Nielsen, Lunde, Shephard, and Veraart (2014), so here we only state them to establish notation for our applied work.

**Example 4** When  $\pi$  has a single atom of support at  $\lambda > 0$ , this is the exponential trawl

$$\begin{aligned} d(s) &= b + (1-b) \exp(\lambda s), \quad s \leq 0, \\ leb(A) &= \frac{1-b}{\lambda}, \quad leb(A_t \cap A) = \frac{1-b}{\lambda} e^{-\lambda t}. \end{aligned} \quad (8)$$

Trivially it only allows short memory as  $\int_0^\infty \bar{\lambda}^{-2} \pi(d\bar{\lambda}) = \lambda^{-2} < \infty$  whenever  $\lambda > 0$ .  $\diamond$

**Example 5** When

$$\pi(d\lambda) = b + (1-b) \frac{\alpha^H}{\Gamma(H)} \lambda^{H-1} e^{-\lambda\alpha} d\lambda, \quad \alpha > 0, \quad H > 1,$$

we produce the superposition gamma (sup- $\Gamma$ ) trawl

$$\begin{aligned} d(s) &= b + (1-b) \left(1 - \frac{s}{\alpha}\right)^{-H}, \quad s \leq 0, \\ leb(A) &= (1-b) \frac{\alpha}{H-1}, \quad leb(A_t \cap A) = \frac{(1-b)\alpha}{H-1} \left(1 + \frac{t}{\alpha}\right)^{1-H}, \quad t \geq 0. \end{aligned} \quad (9)$$

It has long memory when  $H \in (1, 2]$  and short memory when  $H > 2$  as

$$\int_0^\infty \lambda^{-2} \pi(d\lambda) = \frac{\Gamma(H-2)}{\Gamma(H)} < \infty \text{ if and only if } H > 2.$$

$\diamond$

**Example 6** When

$$\pi(d\lambda) = b + (1-b) \frac{(\gamma/\delta)^\nu}{2K_\nu(\gamma\delta)} \lambda^{\nu-1} e^{-(\gamma^2\lambda + \delta^2\lambda^{-1})/2} d\lambda, \quad \gamma, \delta > 0, \quad \nu \in \mathbb{R},$$

we produce the superposition generalized inverse Gaussian (sup-GIG) trawl

$$\begin{aligned}
d(s) &= b + (1-b) \left(1 - \frac{2s}{\gamma^2}\right)^{-\nu/2} \frac{K_\nu(\gamma\delta\sqrt{1-2s/\gamma^2})}{K_\nu(\gamma\delta)}, \quad s \leq 0 \\
leb(A) &= (1-b) \frac{\gamma K_{\nu-1}(\gamma\delta)}{\delta K_\nu(\gamma\delta)}, \\
leb(A_t \cap A) &= (1-b) \frac{\gamma (1+2t/\gamma^2)^{(1-\nu)/2} K_{\nu-1}(\gamma\delta\sqrt{1+2t/\gamma^2})}{\delta K_\nu(\gamma\delta)}, \quad t \geq 0,
\end{aligned} \tag{10}$$

where  $K_\nu(x)$  is the modified Bessel function of the 2nd kind. It always has short memory as

$$\int_0^\infty \lambda^{-2} \pi(d\lambda) = \frac{(\gamma/\delta)^\nu}{2K_\nu(\gamma\delta)} \frac{2K_{\nu-2}(\gamma\delta)}{(\gamma/\delta)^{\nu-2}} = \left(\frac{\gamma}{\delta}\right)^2 \frac{K_{\nu-2}(\gamma\delta)}{K_\nu(\gamma\delta)} < \infty \text{ for all } \gamma, \delta > 0, \nu \in \mathbb{R}.$$

However, it can also degenerate to the long memory sup- $\Gamma$  trawl by letting  $\gamma = \sqrt{2\alpha}$ ,  $\nu = H$  and  $\delta \rightarrow 0$ . When  $\gamma \rightarrow 0$ ,  $\pi(d\lambda)$  becomes an inverse gamma distribution with scale parameter  $\delta^2/2$  and shape parameter  $-\nu$ , so correspondingly we produce the superposition inverse gamma (sup- $\Gamma^{-1}$ ) trawl. This is an important case, for inverse gamma densities have polynomial decay in their tails so will generate short but substantial memory, which has the same pattern as the empirical data. We will see this clearly in Section 5.  $\diamond$

## 4 Moment-based inference

Here we discuss the inference technique based on matching moments using a path of prices  $P_t$ ,  $t \in [0, T]$ . Due to (i) the stationarity of the price changes  $P_\delta - P_0 \stackrel{d}{\sim} P_{t+\delta} - P_t$  for any  $t, \delta$  and (ii) the high frequency nature of the data, moment-based estimates are plausible. The inference can basically split in two pieces: the inference of the Lévy measure  $\nu$  and the inference on  $b$  and  $d$ .

### 4.1 Inference of Lévy measure

Due to the high frequency nature of the data, the instantaneous jumping distribution of the sample is close to the true value. Similarly, the sample power variation  $\{P\}_t^{[r]}$  for any  $r \geq 0$ , when treated as a linear function of time  $t$ , has a slope that is also close to the truth. We can then use these facts to estimate the Lévy measure  $\nu$  in terms of  $b$ .

Let us write the sample instantaneous jumping distribution as  $\hat{\alpha}_y$ , where  $\sum_{y \in \mathbb{Z} \setminus \{0\}} \hat{\alpha}_y = 1$ ; also, estimate the slope of the  $r$ -th sample power variation against  $t$  by

$$\hat{\beta}_r \triangleq \frac{\{P\}_T^{[r]}}{T} = \frac{1}{T} \sum_{0 < t \leq T} |\Delta P_t|^r.$$



Then by matching moments to equations (3) and (4), we should have

$$(2-b) \sum_{y \in \mathbb{Z} \setminus \{0\}} |y|^r \nu(y) = \hat{\beta}_r, \quad r \geq 0, \quad (11)$$

$$\nu(y) + \nu(-y)(1-b) = (2-b) \hat{\alpha}_y \|\nu\|, \quad y \in \mathbb{Z} \setminus \{0\}. \quad (12)$$

Using (11) with the case of  $r = 0$ , we have  $\|\nu\| = \sum_{y \in \mathbb{Z} \setminus \{0\}} \nu(y) = \hat{\beta}_0 / (2-b)$  and hence

$$\begin{aligned} \nu(y) + \nu(-y)(1-b) &= \hat{\alpha}_y \hat{\beta}_0, \\ \nu(-y) + \nu(y)(1-b) &= \hat{\alpha}_{-y} \hat{\beta}_0, \quad y \in \mathbb{N}. \end{aligned}$$

Solving these two equations gives us

$$\widehat{\nu}(y) \triangleq \frac{\hat{\alpha}_y - (1-b) \hat{\alpha}_{-y}}{(2-b)b} \hat{\beta}_0, \quad y \in \mathbb{Z} \setminus \{0\}. \quad (13)$$

**Remark 10** This does not guarantee that  $\widehat{\nu}(y) \geq 0$ , so empirically we will truncate negative  $\widehat{\nu}(y)$  by zero and at the same time tune the value of the corresponding  $\widehat{\nu}(-y)$  such that

$$\widehat{\nu}(y) + \widehat{\nu}(-y) = \frac{\hat{\alpha}_y - (1-b) \hat{\alpha}_{-y} + \hat{\alpha}_{-y} - (1-b) \hat{\alpha}_y}{(2-b)b} \hat{\beta}_0 = \frac{\hat{\alpha}_y + \hat{\alpha}_{-y}}{(2-b)} \hat{\beta}_0$$

remains unchanged. The advantage of this modification allows the conservation of all the (non-negative) moments of the estimated Lévy measure  $\hat{\nu}$ :

$$\sum_{y \in \mathbb{Z} \setminus \{0\}} |y|^r \widehat{\nu}(y) = \sum_{y=1}^{\infty} |y|^r \left( \widehat{\nu}(y) + \widehat{\nu}(-y) \right).$$

However, it comes with the price that the estimates for all of the *odd* cumulants of  $P_t - P_0$  are altered, but practically this will be neglectable as the truncation is only needed for larger  $y$  and the corresponding intensity  $\nu(y)$  is usually quite small.

To completely avoid the negative estimates, one might parameterize the Lévy measure as in Barndorff-Nielsen, Lunde, Shephard, and Veraart (2014), but here we prefer to stay with the non-parametric estimates.  $\diamond$

**Remark 11** We should note that (13) has included all the information we can access from equations (11) and (12), so we cannot rely on equations (11) and (12) to solve  $b$  and the Lévy measure  $\nu$  at the same time. The details can be found in the Appendix A.  $\diamond$

## 4.2 Inference of permanence and trawl function

We will need to employ additional moment equations to estimate the trawl function  $d$  as well as  $b$ . The easiest way to do this is through Theorem 1. In particular, we will use the sample variance of  $\{P_{k\delta} - P_{(k-1)\delta}\}_{k=1}^{T/\delta}$  to estimate

$$\text{Var}(P_\delta - P_0) = (b\delta + 2leb(A_\delta \setminus A_0)) \kappa_2(L_1) = (b\delta + 2leb(A_\delta \setminus A_0)) \sum_{y \in \mathbb{Z} \setminus \{0\}} y^2 \nu(y).$$

Denote the sample variance with the sampling interval  $\delta$  as  $\widehat{\sigma}_\delta^2$ . Then by (13) and matching moments, we should have

$$\widehat{\sigma}_\delta^2 = \left( \frac{b\delta + 2leb(A_\delta \setminus A_0)}{2 - b} \right) \sum_{y \in \mathbb{Z} \setminus \{0\}} y^2 \hat{\alpha}_y \hat{\beta}_0. \quad (14)$$

Appendix D shows how to non-parametrically estimate the trawl function  $d$  using  $\widehat{\sigma}_\delta^2$ , but here we only demonstrate the inference for a parameterized trawl.

Suppose for now that the trawl function  $d$  is parameterized by  $\phi$ , for example,  $\phi = \lambda$  in the exponential trawl (8),  $\phi = (\alpha, H)^T$  in the sup- $\Gamma$  trawl (9) and  $\phi = (\gamma, \delta, \nu)^T$  in the sup-GIG trawl (10). A simple way to estimate  $b$  and  $\phi$  simultaneously is through a non-linear least square fitting to equation (14) divided by  $\delta$  across different  $\delta$ . The reason to work on  $\widehat{\sigma}_\delta^2/\delta$  instead of  $\widehat{\sigma}_\delta^2$  is to amplify the effect of empirical market microstructure for small  $\delta$ , so the non-linear least square estimation of  $b$  and  $\phi$  will not be overly dominated by the linear part of the variogram.

**Remark 12** By definition of the sample variance and the realized variance, as  $T \rightarrow \infty$ ,

$$\begin{aligned} \widehat{\sigma}_\delta^2 &\approx \frac{1}{T/\delta} \sum_{k=1}^{T/\delta} (P_{k\delta} - P_{(k-1)\delta})^2 - \left( \frac{P_T - P_0}{T/\delta} \right)^2, \\ \frac{\widehat{\sigma}_\delta^2}{\delta} &\approx \frac{1}{T} RV^{(T/\delta)} - \delta \frac{(P_T - P_0)^2}{T^2} \approx \frac{1}{T} RV^{(T/\delta)}, \end{aligned}$$

where we throw out the second-order term in the final approximation. Thus, essentially what we try to fit is the variance signature plot ( $RV^{(T/\delta)}$  against  $\delta$ ). From now on, we also call the plot  $\widehat{\sigma}_\delta^2/\delta$  against  $\delta$  a variance signature plot.  $\diamond$

**Example 7** To check the effectiveness of this moment estimator, we conduct a Monte Carlo simulation study on the price process model parameterized by the exponential trawl (8). Throughout the rest of this paper, all the numerical values are reported under the time unit being a second. Then we set  $\lambda_{\text{true}} = 0.681$  and a non-symmetric Skellam basis with Lévy measure

$$\nu(dy) = \nu^+ \delta_{\{1\}}(dy) + \nu^- \delta_{\{-1\}}(dy),$$

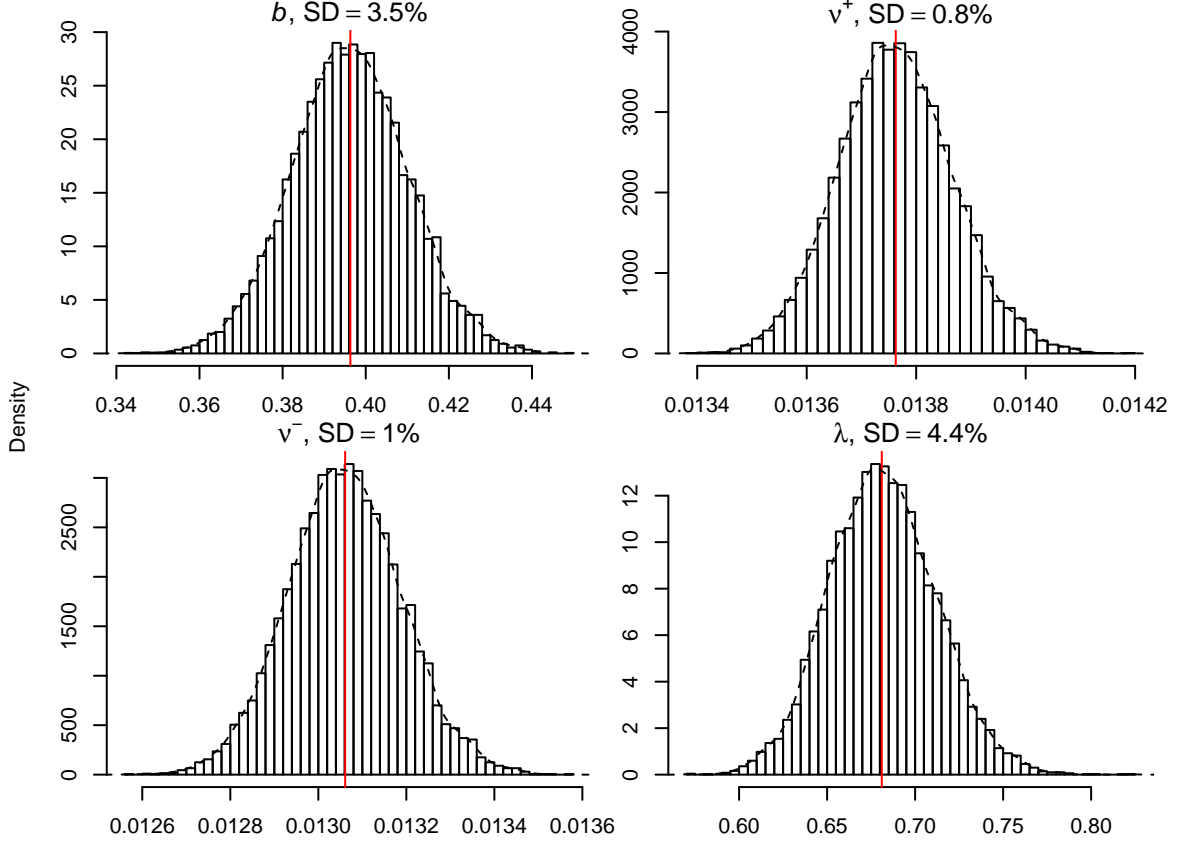


Figure 3: 10,000 Monte Carlo simulation of moment estimations for the price process with exponential trawl  $d(s) = b + (1 - b) \exp(\lambda s)$  and the Skellam basis  $\nu(dy) = \nu^+ \delta_{\{1\}}(dy) + \nu^- \delta_{\{-1\}}(dy)$ . The vertical lines in each of the histograms mean the true value. The Monte Carlo standard deviations are reported on the scale of the true values. Code: `Moment_Inference_ModelBasedBootstrap.R`.

where  $\nu_{\text{true}}^+ = 0.0138$ ,  $\nu_{\text{true}}^- = 0.0131$  and  $b_{\text{true}} = 0.396$ . All the 10,000 Monte Carlo simulated paths are drawn with  $V_0 = 7,486$  (ticks) during the time interval 72,03 to 75,600 (seconds), where 75,600 means the closing time of the market, 21:00. All the settings here are taken from the empirical TNC1006 data set on March 22, 2010, which we will study in next Section.

The non-linear least square fitting for (14) is conducted for  $\delta$ 's ranging from 0.1 seconds to 60 seconds with 60 equally spaced grid points on its log-scale. We then repeat the moment-based estimates for  $\theta = (b, \nu^+, \nu^-, \lambda)^T$  and derive histograms of these estimates in Figure 3. The estimates from the proposed methodology (using equations (13) and (14)) correctly center around the true values; also notice that this method is particularly accurate for estimating  $\nu^+$  and  $\nu^-$ .  $\diamond$

**Remark 13** Except the moment-based estimations, we can also conduct maximum likelihood estimation for our proposed model, which requires sophisticated techniques to filter out the Lévy process  $L(B_t)$ . We are currently exploring particle methods toward this direction.  $\diamond$

## 5 Empirical analysis for futures data

In this Section, we employ these moment-based estimators for empirical analysis. Covering two days of trading activities on two different assets, four data sets are studied here: (i) the Ten-Year US Treasury Note futures contract delivered in June 2010 (TNC1006) during March 22, 2010; (ii) the International Monetary Market (IMM) Euro-Dollar Foreign Exchange (FX) futures contract delivered in June 2010 (EUC1006) during March 22, 2010; (iii) TNC1006 during May 7, 2010; (iv) EUC1006 during May 7, 2010. These data sets come from the same database that is used by Barndorff-Nielsen, Pollard, and Shephard (2012). The first trading day is randomly chosen, while the second trading day is not only the release of US non-farm payroll numbers but was also experiencing the European sovereign debt crisis. These data sets are derived from data feeds at the Chicago Mercantile Exchange (CME). They have been preprocessed using the procedures described in Appendix C. From now on, we will no longer mention the delivery date of each data set and the year 2010.

### 5.1 Data features

All of these four data sets use all the trades from 00:00 to 21:00, shown in Figure 4. With such large time scales, each of the trace plots look like a continuous time diffusion process. However, if we focus these data sets to much smaller time scales (within one hour for TNC and within two minutes for EUC), shown in Figure 5, the discreteness becomes important. In particular, we can see several multiple-tick jumps in the two EUC data sets shown in Figure 5.

Table 1 summarizes some basic features of these four data sets. Both contracts have more

Contract, Day	Tick Size (\$)	Num. of Price Changes	Size of Price Changes (Tick)			
			Avg.	SD.	Min.	Max.
TNC, 03/22	1/64	3,249	0.00646	1.000	-1	1
EUC, 03/22	0.0001	13,943	0.00337	1.012	-2	3
TNC, 05/07	1/64	12,849	-0.000467	1.035	-13	15
EUC, 05/07	0.0001	55,379	0.00190	1.077	-13	15

Table 1: Summary statistics of the four futures data sets.

activities during May 7 than during March 22 and the standard deviations of the jump size for all the four data sets are close to 1 even though the range of all possible jump sizes might differ a lot.

We also plot the empirical instantaneous jumping distribution (on the log-scale) for the four data sets in Figure 6. Those estimated probabilities will be used as  $\hat{\alpha}_y$  for the moment estimate defined in the previous Section. Generally, the jumps of EUC have more variability than the TNC.

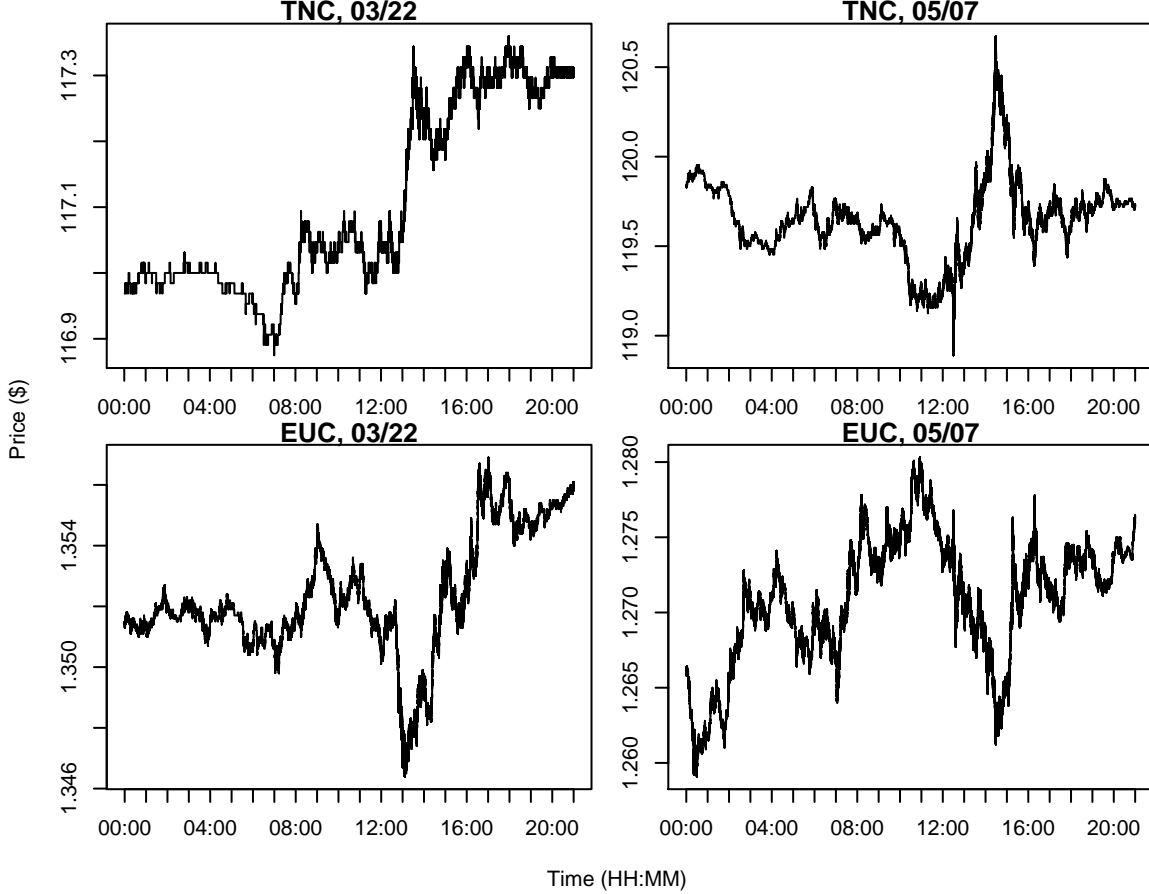


Figure 4: The complete trace plots for the four data sets during 00:00 to 21:00. The  $x$ -axis is the calendar time (HH:MM), while the  $y$ -axis is the price (\$). Code: `Price_Plots.R`.

Furthermore, we can see that even for the same contract, say TNC, the jumping characteristic is completely different from a random chosen day (March 22) to a day with a major economic event (May 7). In a normal day like March 22, the TNC trading has depths so large that it always jumps by one tick, but the situation changes enormously for a highly active day like May 7, by this time the TNC trading behaves just like other multiple-tick markets.

**Remark 14** One more implication from Figure 6 is that  $\kappa_1(L_1)$  is, of course, a small number. To see this, we note that

$$\widehat{\kappa_1(L_1)} = \sum_{y \in \mathbb{Z} \setminus \{0\}} y \widehat{\nu}(y) = \frac{\sum_{y \in \mathbb{Z} \setminus \{0\}} y \hat{\alpha}_y - (1-b) \sum_{y \in \mathbb{Z} \setminus \{0\}} y \hat{\alpha}_{-y}}{(2-b)b} \hat{\beta}_0 = \frac{\sum_{y \in \mathbb{Z} \setminus \{0\}} y \hat{\alpha}_y}{b} \hat{\beta}_0.$$

Hence, the more symmetric the Figure 6, the smaller the estimate of  $\kappa_1(L_1)$ .  $\diamond$

Finally, we show the correlograms of the four data sets in Figure 7, using three orders of magnitude of sampling intervals  $\delta$ : 0.1 second, 1 second, 10 seconds and 1 minute. For each

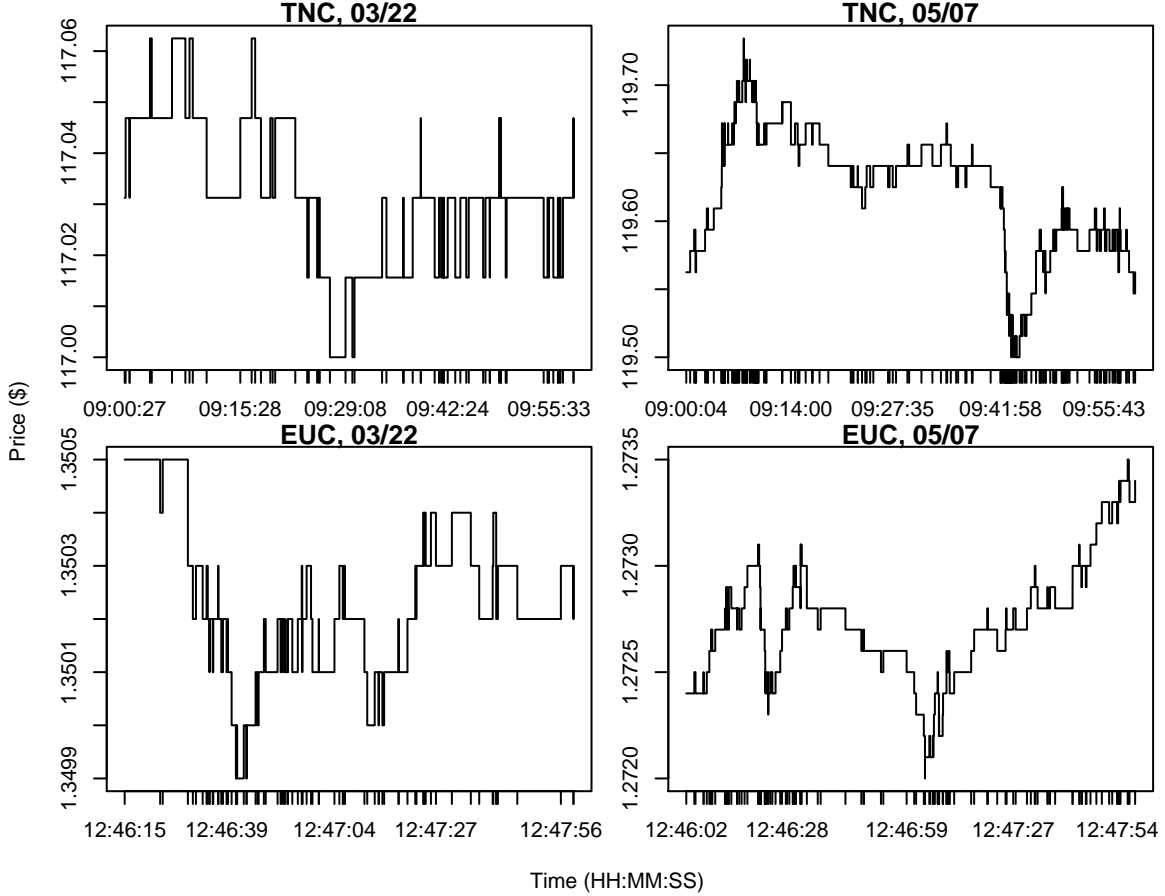


Figure 5: The trace plots for two TNC data sets during 09:00 to 10:00 and for two EUC data sets during 12:46 to 12:48. The  $x$ -axis is the calendar time (HH:MM:SS), while the  $y$ -axis is the price (\$). Code: Price\_Plots.R.

data set, we will use a single set of parameters in our price model to fit all of the correlograms with different  $\delta$ . In general, these autocorrelations are significantly negative and increasing as  $k$  increases, while if  $\delta$  gets very large the autocorrelations will fall to roughly zero. Of course there is strong evidence that the empirical data cannot be well-described by a pure Lévy process, which always gives zero autocorrelations for returns. Our model is capable of describing these autocorrelation features (Theorem 3 and Corollary 1). The next Subsection conducts moment-based estimations for these empirical data sets.

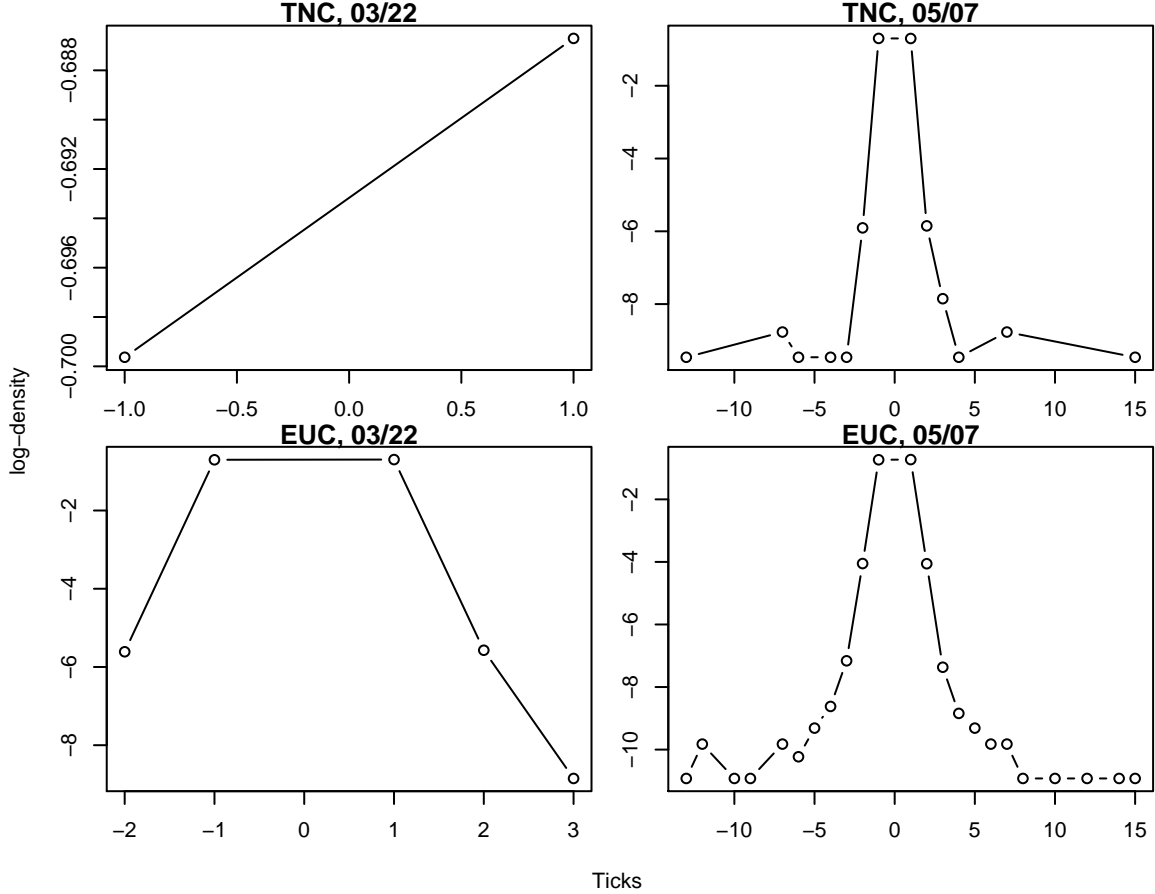


Figure 6: The log-histograms for the empirical instantaneous jumping distributions of the four data sets. The  $x$ -axis for each plot is the size of the jump, while the  $y$ -axis denotes the estimated probability value in a log-scale. Code: `Price_Plots.R`.

## 5.2 Parameter estimation

We use the methodology described before on the four data sets with the three different trawls (8), (9) and (10). The estimation<sup>5</sup> results are shown in Table 2 on page 25, where

$$\nu^+ \triangleq \sum_{y=1}^{\infty} \nu(y) \quad \text{and} \quad \nu^- \triangleq \sum_{y=1}^{\infty} \nu(-y)$$

are the positive and negative jump intensities respectively. We observe in the Table that the estimation of  $\nu^+$  and  $\nu^-$  are relatively robust across different choices of trawls. The estimate of  $H$  in Table 2 clearly suggests the insufficiency of using a sup- $\Gamma$  trawl for the empirical data. Furthermore, even though we fit a more general sup-GIG trawl with three parameters, the four empirical data sets can almost be described by the sup- $\Gamma^{-1}$  trawl with only two parameters (the

<sup>5</sup>To especially emphasize the fitting of market microstructure effects, the sample variance is calculated on an equally distant grid on the log-scale of  $\delta$  whose range is shown in Figure 9.

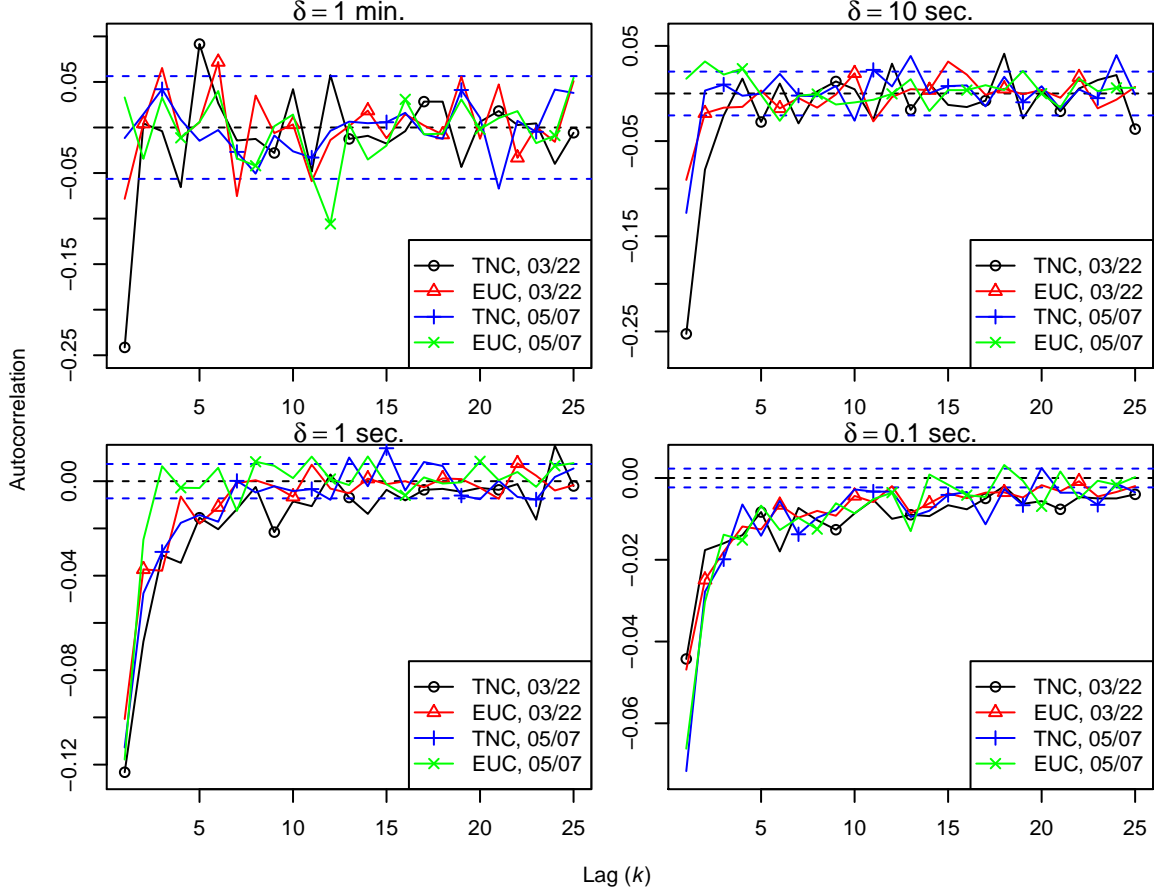


Figure 7: The correlograms with different sampling intervals  $\delta = 0.1, 1, 10, 60$  (seconds) for the four data sets. The  $x$ -axis for each plot is the lag  $k$ , while the  $y$ -axis denotes the value of empirical autocorrelation. The dashed lines are located at  $\pm 2/\sqrt{T/\delta}$ . Code: `PricePlots.R`.

case of  $\gamma \rightarrow 0$  for sup-GIG trawl mentioned in Section 3.6). This phenomenon might be attributed to the fact that inverse gamma distributions decay exponentially near the origin but polynomially near infinity, allowing it to capture these very different time scales.

**Remark 15** In the same Table, we also provide the standard error (SE) estimates for these moment-based estimations using the model-based bootstrap, i.e., a vanilla Monte Carlo simulation with plugged-in parameters.  $\diamond$

Using these estimated parameters, we first show the variance signature plots of  $\widehat{\sigma}_\delta^2/\delta$  against  $\delta$  along with the corresponding theoretical curves (14) for each trawl in Figure 8 and 9, where the second of these graphs uses a log-scale for  $\delta$ . In each of the plots, we put not only  $\lim_{\delta \rightarrow 0} \widehat{\sigma}_\delta^2/\delta = \left(\partial_\delta \widehat{\sigma}_\delta^2\right)(0) = \sum_{y \in \mathbb{Z} \setminus \{0\}} y^2 \hat{\alpha}_y / \hat{\beta}_0$  at the corresponding location of  $\delta = 0$  but also a reference horizontal line from a pure Lévy process model ( $b = 1$ ), which is calculated from the slope of a linear fitting



Trawl	Para	TNC, 03/22		EUC, 03/22		TNC, 05/07		EUC, 05/07	
		Est.	SE	Est.	SE	Est.	SE	Est.	SE
Exp	$b$	0.396	0.014	0.654	0.008	0.574	0.015	0.694	0.007
	$\nu^+$	0.014	0.000	0.069	0.000	0.059	0.001	0.282	0.001
	$\nu^-$	0.013	0.000	0.068	0.000	0.060	0.001	0.279	0.001
	$\lambda$	0.681	0.030	2.470	0.083	3.888	0.218	4.033	0.133
sup- $\Gamma$	$b$	0.283	0.021	0.604	0.012	0.525	0.016	0.649	0.010
	$\nu^+$	0.013	0.000	0.067	0.001	0.057	0.001	0.272	0.002
	$\nu^-$	0.012	0.000	0.066	0.001	0.058	0.001	0.270	0.002
	$\alpha$	1.146	0.191	0.311	0.037	0.187	0.038	0.192	0.023
	$H$	1.000	0.125	1.000	0.104	1.000	0.139	1.000	0.102
sup-GIG	$b$	0.186	0.028	0.528	0.034	0.440	0.029	0.648	0.011
	$\nu^+$	0.013	0.000	0.063	0.001	0.054	0.001	0.272	0.002
	$\nu^-$	0.011	0.000	0.062	0.001	0.055	0.001	0.269	0.002
	$\gamma$	0.000	0.066	0.000	0.030	0.003	0.028	0.000	0.064
	$\delta$	0.453	0.049	0.604	0.085	0.583	0.099	1.525	0.209
	$\nu$	-0.604	0.078	-0.453	0.067	-0.332	0.077	-0.741	0.170

Table 2: Moment-based estimations under different trawls for the four data sets. Also shown are the standard error (SE) estimates for the moment estimator to each parameter using the model-based bootstrap, where the number of bootstrapped paths we draw is 10,000.

line in the variogram of  $\widehat{\sigma}_g^2$  against  $\delta$ .

These fittings to the variance signature plots show good results—here we particularly notice that using a sup-GIG trawl gives a very good fit; while the other two simpler trawls fail to fit the region with a smaller  $\delta$ . This point becomes apparent when we check Figure 9.

To further examine our model fitting, we also show the log-histograms for the return distribution with different  $\delta$  along with the theoretical curves (by applying the inverse Fourier transform on Theorem 1) in Figure 10. For a larger  $\delta$  the sup-GIG trawl do a better job than the other two trawls (not shown in Figure 10) while for a smaller  $\delta$  the difference among the three trawls is limited. As an overall comment, our model seems to underestimate the tail part of each of the empirical jumping distributions.

We now demonstrate the correlograms for the returns with different  $\delta$  along with the theoretical curves in Figure 11. For a larger  $\delta$ , the empirical returns look almost uncorrelated (insignificant from being 0) except for TNC on March 22, but the sup-GIG trawl still captures this anomaly at the first lag. As  $\delta$  becomes smaller, those negative correlations become more significant; even though the exponential trawl and the sup- $\Gamma$  trawl (not shown in Figure 11) can depict the shape of the autocorrelation, only sup-GIG trawl can fit the first few lags.

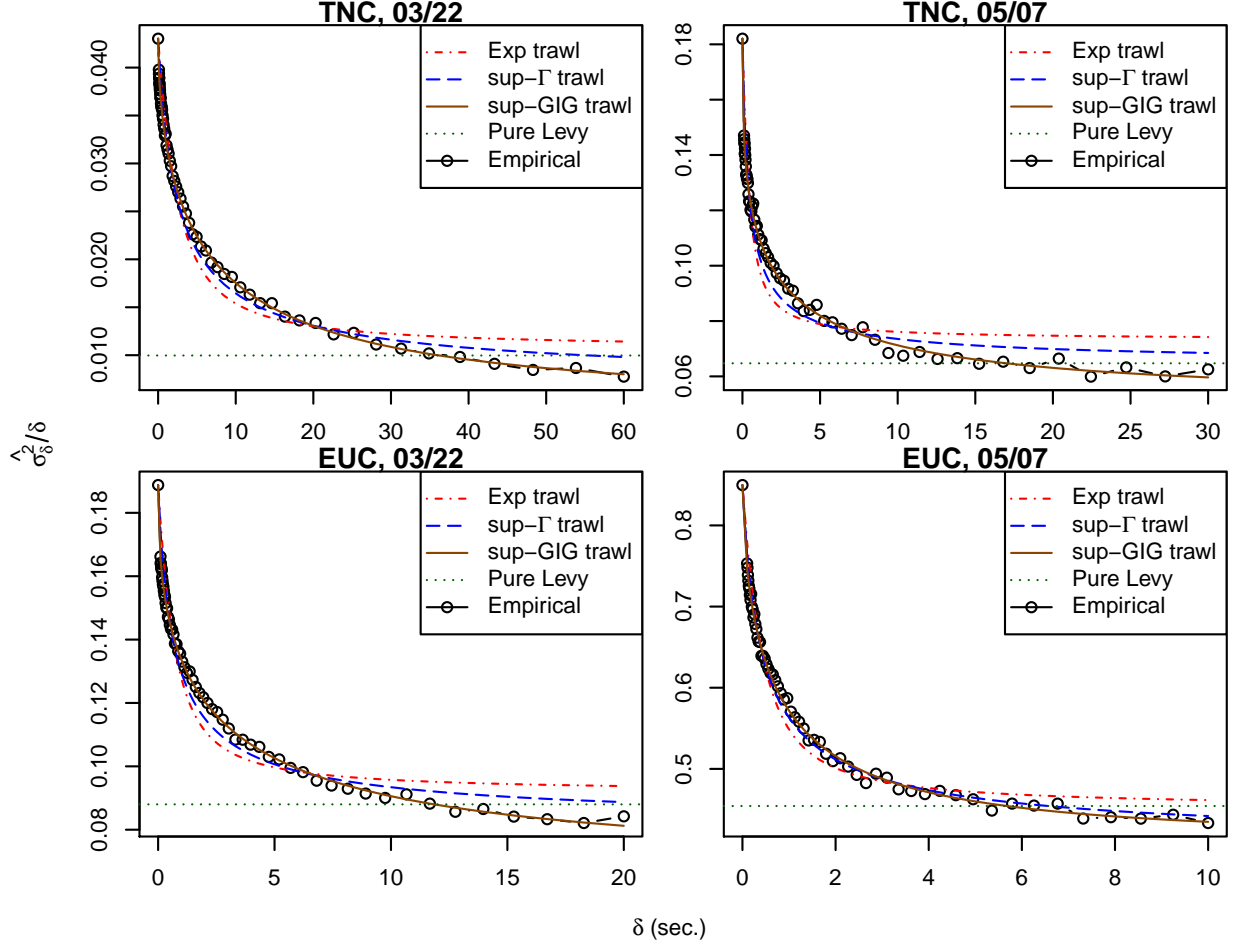


Figure 8: The variance signature plots for the four data sets along with the fitting curves from different trawls. The  $x$ -axis for each plot is  $\delta$  (seconds), while the  $y$ -axis denotes the value of the sample variance of returns divided by  $\delta$ . Code: `Moment_Inference_v2.0.R`.

As a summary, the sup-GIG trawl (or essentially the sup- $\Gamma^{-1}$  trawl) performs better than the other two trawls in every aspects. These empirical analyses demonstrate the descriptive power of our proposed model for the futures data.

**Remark 16** We now criticize the insufficient part of our proposed model. A plot (not shown) of the counting process of price moves for our four data sets will clearly show a non-linear increasing pattern that disobeys the linearity described by equation (4). This non-linear pattern can be attributed to the well-known diurnal time-varying levels of trading activity. For the same contract, its two counting process plots look alike (after rescaling) across different trading days.

We are currently exploring methods that can adjust the model to deal with these effects, hoping to report on them shortly. It will involve the use of two independent stochastic time changes for the positive events and the negative events. A special case on the Skellam Lévy process using this

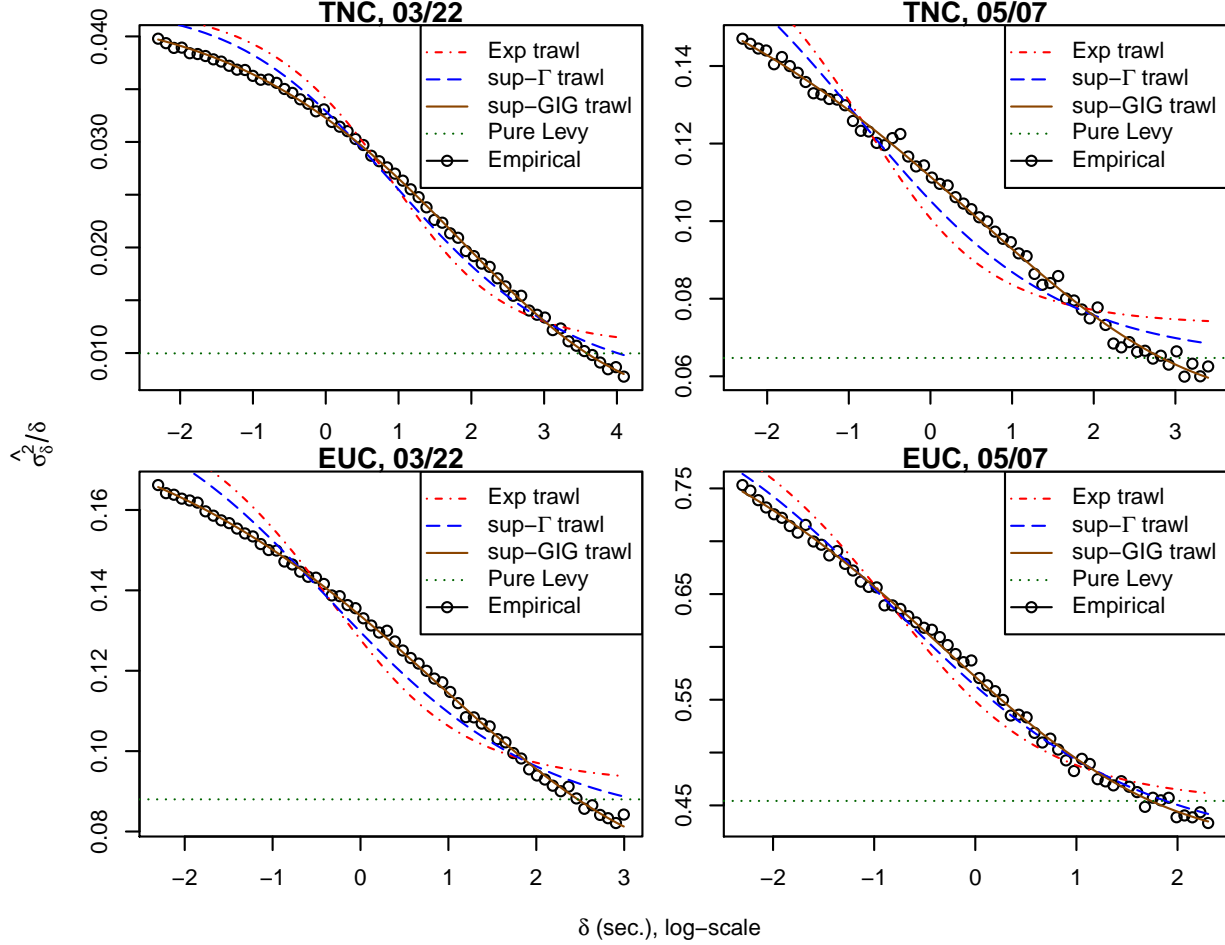


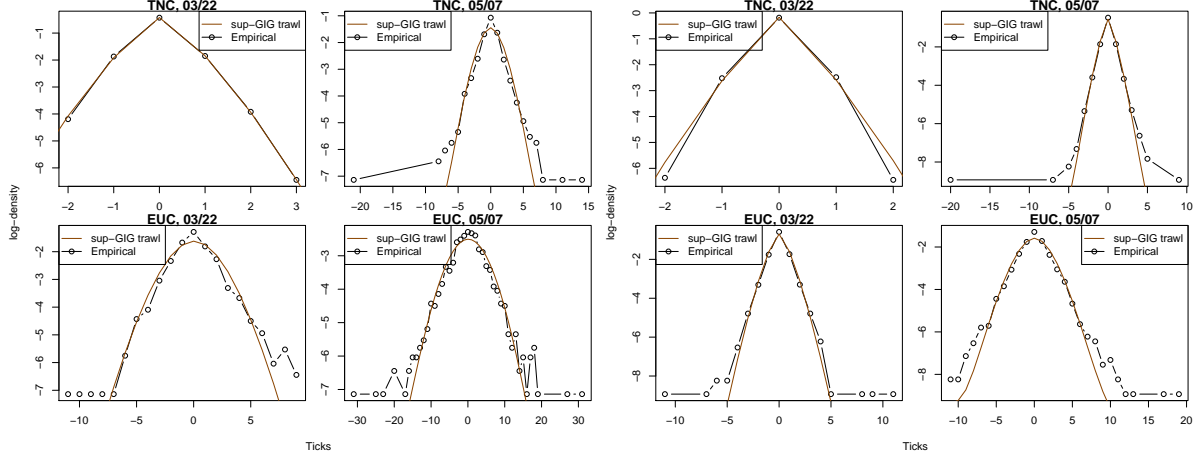
Figure 9: The variance signature plots for the four data sets along with the fitting curves from different trawls in the scale of  $\log \delta$ . Code: `Moment_Inference_v2.0.R`.

ideas has been addressed in Kerres, Leonenko, and Sikorskii (2014).  $\diamond$

## 6 Conclusion

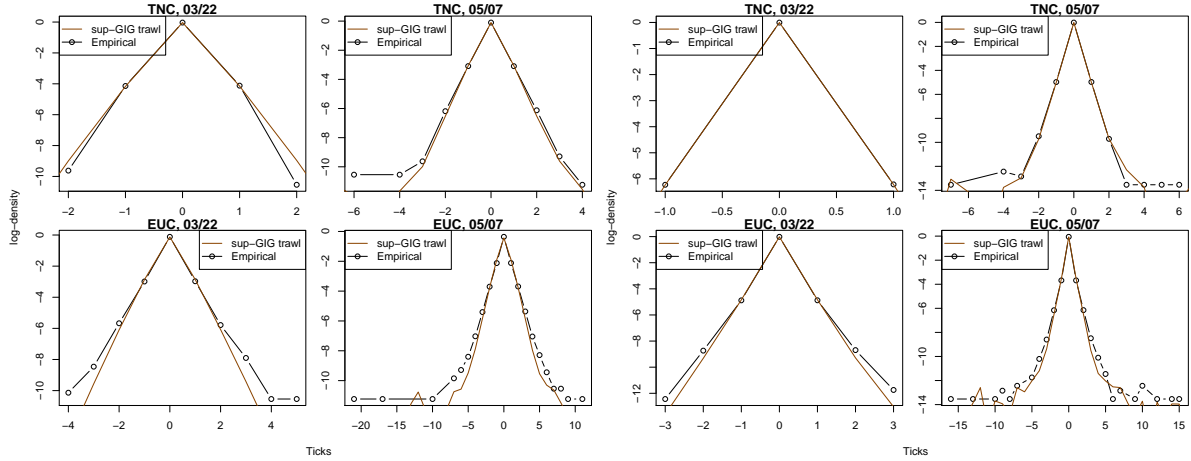
We propose a novel and simple model that can adequately capture some of the important features of high frequency financial data. It is able to deal with the dependence in price changes measured over three different orders of magnitude of time intervals. The model is directly formulated in terms of the price impact curve (or trawl function). It has a càdlàg price process that is a piecewise constant semimartingale with finite activity, finite variation and no Brownian motion component.

However, we need to emphasize that, the proposed model in this paper is just an initial step. Even though we emphasize the discreteness and the fleetingness in the movements of the price process, we have been assuming a simple structure so far with no time-varying features. We



(a)  $\delta = 60$  seconds.

(b)  $\delta = 10$  seconds.



(c)  $\delta = 1$  second.

(d)  $\delta = 0.1$  seconds.

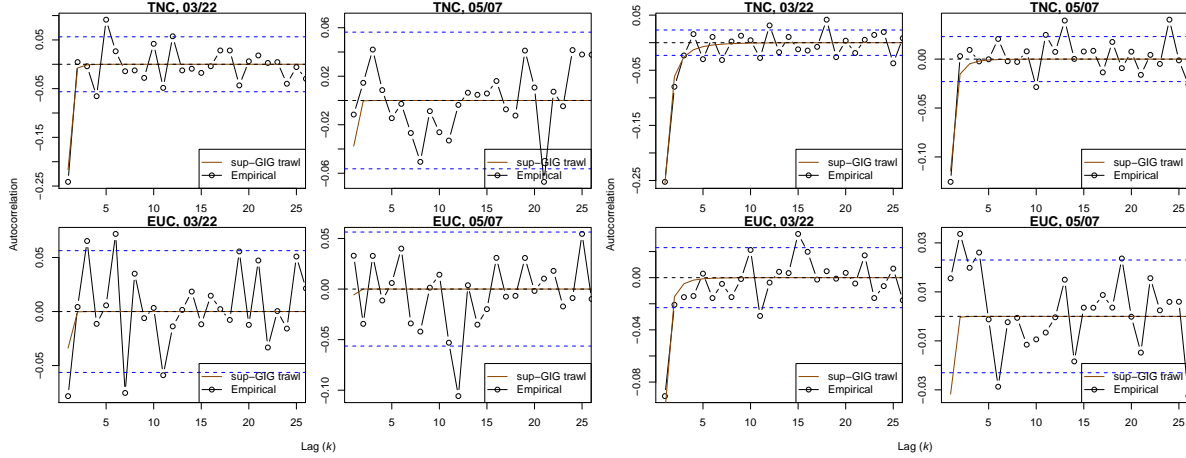
Figure 10: The log-histograms for the returns of the four data sets over several sampling intervals along with the theoretical curves from sup-GIG trawl. Code: `Moment_Inference_v2.0.R`.

will shortly report on how to generalize this model to the more realistic case using a stochastic time-change.

Our model provides a good description to the empirical data, while we majorly focus on the trade prices, which is not always immediately tradable. For market practitioners who sit either on the buy side or the sell side, they might consider to apply the proposed model on either the ask price or bid price, so our model is much more widely applicable than the cases we report here.

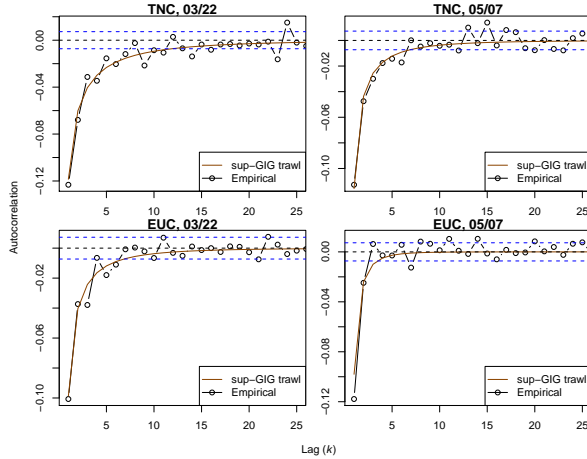
## 7 Acknowledgements

We thank Mikkel Bennesen, Per Mykland, Mikkel Plagborg-Møller, Almut Veraart, Shihao Yang and various seminar groups for their comments on an earlier draft.

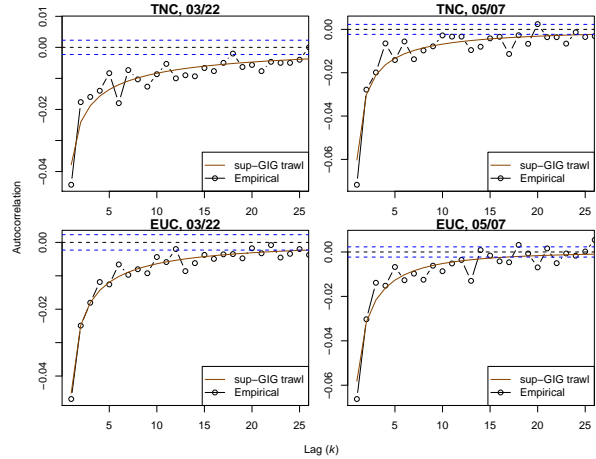


(a)  $\delta = 60$  seconds.

(b)  $\delta = 10$  seconds.



(c)  $\delta = 1$  second.



(d)  $\delta = 0.1$  seconds.

Figure 11: The correllograms for the returns of the four data sets over several sampling intervals along with the theoretical curves from sup-GIG trawl. The dashed lines are located at  $\pm 2/\sqrt{T/\delta}$ . Code: `Moment_Inference_v2.0.R`.

## References

- Andersen, T. G., T. Bollerslev, F. X. Diebold, and P. Labys (2001). The distribution of exchange rate volatility. *Journal of the American Statistical Association* 96, 42–55.
- Bacry, E., S. Delattre, M. Hoffman, and J. F. Muzy (2013a). Modelling microstructure noise with mutually exciting point processes. *Quantitative Finance* 13, 65–77.
- Bacry, E., S. Delattre, M. Hoffman, and J. F. Muzy (2013b). Some limit theorems for Hawkes processes and application to financial statistic. *Stochastic Processes and their Applications* 123, 2475–2499.
- Ball, C. A. (1988). Estimation bias induced by discrete security pricing. *Journal of Finance* 43, 841–865.
- Ball, C. A., W. N. Torous, and A. E. Tschoegl (1985). The degree of price resolution: The case of the gold market. *Journal of Futures Markets* 5, 29–43.
- Barndorff-Nielsen, O. E., P. R. Hansen, A. Lunde, and N. Shephard (2008). Designing realised kernels to measure the ex-post variation of equity prices in the presence of noise. *Econometrica* 76, 1481–1536.
- Barndorff-Nielsen, O. E., A. Lunde, N. Shephard, and A. E. D. Veraart (2014). Integer-valued trawl processes: A class of stationary infinitely divisible processes. *Scandinavian Journal of Statistics* 41,

- Barndorff-Nielsen, O. E., D. G. Pollard, and N. Shephard (2012). Integer-valued Lévy processes and low latency financial econometrics. *Quantitative Finance* 12, 587–605.
- Barndorff-Nielsen, O. E. and N. Shephard (2002). Econometric analysis of realised volatility and its use in estimating stochastic volatility models. *Journal of the Royal Statistical Society, Series B* 64, 253–280.
- Barndorff-Nielsen, O. E. and N. Shephard (2004). Power and bipower variation with stochastic volatility and jumps (with discussion). *Journal of Financial Econometrics* 2, 1–48.
- Bartlett, M. S. (1978). *An Introduction to Stochastic Processes, with Special Reference to Methods and Applications* (3 ed.). Cambridge: Cambridge University Press.
- Bowsher, C. G. (2007). Modelling security market events in continuous time: Intensity based, multivariate point process models. *Journal of Econometrics* 141, 876–912.
- Cipollini, F., R. F. Engle, and G. Gallo (2009). A model for multivariate non-negative valued processes in financial econometrics. Available at SSRN: <http://ssrn.com/abstract=1333869> or <http://dx.doi.org/10.2139/ssrn.1333869>.
- Delattre, S. and J. Jacod (1997). A central limit theorem for normalized functions of the increments of a diffusion process in the presence of round-off errors. *Bernoulli* 3, 1–28.
- Engle, R. F. (2000). The econometrics of ultra-high frequency data. *Econometrica* 68, 1–22.
- Engle, R. F. and J. R. Russell (1998). Forecasting transaction rates: The autoregressive conditional duration model. *Econometrica* 66, 1127–1162.
- Fauth, A. and C. A. Tudor (2012). Modeling first line of an order book with multivariate marked point processes. *ArXiv e-prints*. Unpublished paper, SAMM, Université Paris 1 Panthéon-Sorbonne, November.
- Fodra, P. and H. Pham (2013a). High frequency trading in a Markov renewal model. *ArXiv e-prints*. Unpublished paper, Laboratoire de Probabilités et, Université Paris 7 Diderot, October.
- Fodra, P. and H. Pham (2013b). Semi Markov model for market microstructure. *ArXiv e-prints*. Unpublished paper, Laboratoire de Probabilités et, Université Paris 7 Diderot, May.
- Fuchs, F. and R. Stelzer (2013). Mixing conditions for multivariate infinitely divisible processes with an application to mixed moving averages and the supOU stochastic volatility model. *ESAIM: Probability and Statistics* 17, 455–471.
- Gottlieb, G. and A. Kalay (1985). Implications of the discreteness of observed stock prices. *Journal of Finance* 40, 135–153.
- Griffin, J. E. and R. C. A. Oomen (2008). Sampling returns for realized variance calculations: Tick time or transaction time? *Econometric Review* 27, 230–253.
- Hamilton, J. D. and O. Jordá (2002). A model of the federal funds rate target. *Journal of Political Economy* 110, 1135–1167.
- Hansen, P. R. and A. Lunde (2006). Realized variance and market microstructure noise (with discussion). *Journal of Business and Economic Statistics* 24, 127–218.
- Harris, L. (1990). Estimation of stock price variances and serial covariances from discrete observations. *Journal of Financial Quantitative Analysis* 25, 291–306.
- Hasbrouck, J. (1999). The dynamics of discrete bid and ask quotes. *Journal of Finance* 54, 2109–2142.
- Hautsch, N. (2012). *Econometrics of Financial High-Frequency Data*. Berlin Heidelberg: Springer.
- Hawkes, A. G. (1972). Spectra of some mutually exciting point processes with associated variables. In P. A. W. Lewis (Ed.), *Stochastic Point Processes*, pp. 261–271. New York: Wiley.
- Jacod, J. (1996). La variation quadratique du Brownien en présence d’erreurs d’arrondi. *Asterisque* 236, 155–162.
- Jacod, J., Y. Li, P. A. Mykland, M. Podolskij, and M. Vetter (2009). Microstructure noise in the continuous case: The pre-averaging approach. *Stochastic Processes and Their Applications* 119, 2249–2276.

- Kerss, A., N. Leonenko, and A. Sikorskii (2014). Fractional Skellam processes with applications to finance. *Fractional Calculus and Applied Analysis* 17, 532–551.
- Kingman, J. F. C. (1993). *Poisson Processes*. New York: Oxford University Press.
- Kolassa, J. and P. McCullagh (1990). Edgeworth series for lattice distributions. *Annals of Statistics* 18, 981–985.
- Large, J. (2011). Estimating quadratic variation when quoted prices jump by a constant increment. *Journal of Econometrics* 160, 2–11.
- Li, Y. and P. A. Mykland (2014). Rounding errors and volatility estimation. *Journal of Financial Econometrics*.
- Liesenfeld, R., I. Nolte, and W. Pohmeier (2006). Modelling financial transaction price movements: a dynamic integer count model. *Empirical Economics* 30, 795–825.
- Lindley, D. V. (1956). The estimation of velocity distributions from counts. In *Proceedings of the International Congress of Mathematicians*, Volume 3, pp. 427–444. Amsterdam: North-Holland.
- Mykland, P. A. and L. Zhang (2012). The econometrics of high frequency data. In M. Kessler, A. Lindner, and M. Sørensen (Eds.), *Statistical Methods for Stochastic Differential Equations*, pp. 109–190. New York: Chapman & Hall/CRC Press. Forthcoming.
- Oomen, R. C. A. (2005). Properties of bias-corrected realized variance under alternative sampling schemes. *Journal of Financial Econometrics* 3, 555–577.
- Oomen, R. C. A. (2006). Properties of realized variance under alternative sampling schemes. *Journal of Business & Economic Statistics* 24, 219–237.
- Press, S. J. (1967). A compound events model for security prices. *Journal of Business* 40, 317–335.
- Reynolds, J. F. (1968). On the autocorrelation and spectral functions of queues. *Journal of Applied Probability* 5, 467–475.
- Rosenbaum, M. (2009). Integrated volatility and round-off error. *Bernoulli* 15, 687–720.
- Russell, J. R. (1999). Econometric modeling of multivariate irregularly-spaced high-frequency data. Unpublished paper, Booth School of Business, University of Chicago.
- Russell, J. R. and R. F. Engle (2006). A discrete-state continuous-time model of financial transaction prices and times. *Journal of Business and Economic Statistics* 23, 166–180.
- Russell, J. R. and R. F. Engle (2010). Analysis of high-frequency data. In Y. Ait-Sahalia and L. P. Hansen (Eds.), *Handbook of Financial Econometrics: Tools and techniques*, pp. 383–426. Amsterdam: North-Holland.
- Rydberg, T. H. and N. Shephard (2003). Dynamics of trade-by-trade price movements: Decomposition and models. *Journal of Financial Econometrics* 1, 2–25.
- Surgailis, D., J. Rosinski, V. Mandrekar, and S. Cambanis (1993). Stable mixed moving averages. *Probability Theory and Related Fields* 97, 543–558.
- Wolpert, R. L. and L. D. Brown (2011). Stationary infinitely-divisible Markov processes with non-negative integer values. Working paper, Department of Statistics, Duke University.
- Wolpert, R. L. and M. S. Taqqu (2005). Fractional Ornstein-Uhlenbeck Lévy processes and the telecom process: Upstairs and downstairs. *Signal Processing* 85, 1523–1545.
- Zhang, L. (2006). Efficient estimation of stochastic volatility using noisy observations: A multi-scale approach. *Bernoulli* 12, 1019–1043.
- Zhang, M. Y., J. R. Russell, and R. Tsay (2001). Determinants of bid and ask quotes and implications for the cost of trading. *Journal of Empirical Finance* 15, 656–678.
- Zhou, B. (1996). High-frequency data and volatility in foreign-exchange rates. *Journal of Business and Economic Statistics* 14, 45–52.

## A Proofs and details

**Details of Remark 2.** To see this, we first argue that  $P_t$  is a semimartingale with respect to the *complete data filtration*  $\mathcal{F}_t \vee \mathcal{S}_t$ , which includes the history of the price process itself ( $\mathcal{F}_t$ ) and the history of all the hidden activities of events ( $\mathcal{S}_t$ ). Precisely,  $\mathcal{S}_t$  is the natural filtration generated by the process of *random set*  $S_t$ , which consists of all the surviving events  $(q, y)$  in the trawl at time  $t$ , where  $q \leq t$  is the original arrival time of the event and  $y$  is its size. Then clearly  $L(A_t) = \sum_{(q,y) \in S_t} y$  is a càdlàg adapted process (w.r.t.  $\mathcal{S}_t$ ) of locally bounded variation if the underlying Lévy basis has finite activities.

Denote the natural filtration generated by the path of  $L(B_t)$  as  $\mathcal{L}_t$ . Then from the definition of  $P_t$  the complete data information  $\mathcal{F}_t \vee \mathcal{S}_t$  must be the same as  $\mathcal{L}_t \vee \mathcal{S}_t \vee \sigma(V_0)$ —the path of  $L(B_t)$  will be completely revealed under  $\mathcal{F}_t \vee \mathcal{S}_t$ , where  $\{\mathcal{L}_t\}$ ,  $\{\mathcal{S}_t\}$  and  $V_0$  are completely independent to each other. Thus,

$$M_t \triangleq L(B_t) - b \left( \sum_{y \in \mathbb{Z} \setminus \{0\}} y \nu(y) \right) t \in \mathcal{L}_t \subseteq \mathcal{F}_t \vee \mathcal{S}_t$$

must be a martingale w.r.t.  $\mathcal{F}_t \vee \mathcal{S}_t$  because

$$\mathbb{E}(M_t | \mathcal{F}_s, \mathcal{S}_s) = \mathbb{E}(M_t | \mathcal{L}_s, \mathcal{S}_s, V_0) = \mathbb{E}(M_t | \mathcal{L}_s) = M_s,$$

where the second equality follows from the independence between  $\{\mathcal{L}_t\}$ ,  $\{\mathcal{S}_t\}$  and  $V_0$ .

Write

$$P_t = M_t + Q_t, \quad Q_t \triangleq V_0 + L(A_t) + b \left( \sum_{y \in \mathbb{Z} \setminus \{0\}} y \nu(y) \right) t.$$

As  $V_0$  can be revealed under  $\mathcal{F}_0$  and  $\mathcal{S}_0$ , it is trivially in  $\mathcal{F}_t \vee \mathcal{S}_t$ , too. Then  $Q_t$  is also a càdlàg adapted process (w.r.t.  $\mathcal{F}_t \vee \mathcal{S}_t$ ) of locally bounded variation. We then conclude that  $P_t$  is a semimartingale w.r.t.  $\mathcal{F}_t \vee \mathcal{S}_t$ . As the property of being a semimartingale is preserved under shrinking the filtration,  $P_t$  is a semimartingale w.r.t.  $\mathcal{F}_t \subseteq \mathcal{F}_t \vee \mathcal{S}_t$ . ■

**Proof of Theorem 1.** We partition  $C_t$  and  $C_0$  into three disjoint sets, one of which is in common:

$$C_t = (C_t \cap C_0) \cup (C_t \setminus C_0), \quad C_0 = (C_t \cap C_0) \cup (C_0 \setminus C_t),$$

so this means that

$$P_t - P_0 = L(C_t \setminus C_0) - L(C_0 \setminus C_t).$$



$L(C_t \setminus C_0)$  is clearly independent of  $L(C_0 \setminus C_t)$  due to the independence property of the Lévy basis and the disjointedness between  $C_t \setminus C_0$  and  $C_0 \setminus C_t$ .

For any  $t \geq 0$ ,

$$\begin{aligned} C_t \setminus C_0 &= (A_t \setminus A) \cup B_t = (A_t \setminus A) \cup ([0, b) \times (0, t]) \\ C_0 \setminus C_t &= A \setminus A_t, \\ leb(C_t \setminus C_0) &= leb(A_t \setminus A) + bt, \\ leb(C_0 \setminus C_t) &= leb(A \setminus A_t) = leb(A_t \setminus A). \end{aligned}$$

Then

$$\begin{aligned} C(\theta \dagger P_t - P_0) &= C(\theta \dagger L(C_t \setminus C_0)) + C(-\theta \dagger L(C_0 \setminus C_t)), \\ &= leb(C_t \setminus C_0)C(\theta \dagger L_1) + leb(C_0 \setminus C_t)C(-\theta \dagger L_1) \\ &= btC(\theta \dagger L_1) + leb(A_t \setminus A)(C(\theta \dagger L_1) + C(-\theta \dagger L_1)). \end{aligned}$$

For any random variable  $X$  we always have

$$\kappa_j(X) = \frac{1}{j!} \frac{\partial^j}{\partial \theta^j} C(\theta \dagger X) \Big|_{\theta=0},$$

so using the equation above it is clear that

$$\kappa_j(P_t - P_0) = (bt + leb(A_t \setminus A)(1 + (-1)^j)) \kappa_j(L_1),$$

which is the required result. ■

**Proof of Theorem 2.** For each  $y \in \mathbb{Z} \setminus \{0\}$ , the price process has a jump with size  $y$  if and only if either one event with size  $y$  arrives or one event with size  $-y$  departures—thanks to the monotonicity of  $d$ . Thus, the probability of the arrival event can be characterized by the non-zero probability of a Poisson random variable with intensity

$$\nu(y) leb(D_t \setminus D_{t-dt}) \approx \nu(y) dt;$$

on the other hand, the probability of the departure event can be similarly depicted by the non-zero probability of a Poisson random variable with intensity

$$\nu(-y) leb(A_{t-dt} \setminus A_t) \approx \nu(-y)(1-b) dt.$$

Therefore, by noting that  $\mathbb{P}(X > 0) = 1 - e^{-\lambda} \approx \lambda$  for  $X \sim \text{Pois}(\lambda)$  and small  $\lambda$ , we have

$$\mathbb{P}(\Delta P_t = y | \Delta P_t \neq 0) = \frac{\mathbb{P}(\Delta P_t = y)}{\sum_{y \in \mathbb{Z} \setminus \{0\}} \mathbb{P}(\Delta P_t = y)}$$

$$\begin{aligned}
&= \frac{\nu(y) dt + \nu(-y)(1-b) dt}{\sum_{y \in \mathbb{Z} \setminus \{0\}} (\nu(y) dt + \nu(-y)(1-b) dt)} \\
&= \frac{\nu(y) + \nu(-y)(1-b)}{(2-b) \|\nu\|}.
\end{aligned}$$

■

**Proof of Theorem 3.** We will use the following straightforward result on the increments of a process to prove Theorem 3.

**Lemma 1** *Suppose that  $Z_t$ , for  $t \in \mathbb{R}$ , has covariance stationary increments. Then for  $\delta > 0$  and  $k = 1, 2, 3, \dots$*

$$\begin{aligned}
\gamma_k &\triangleq \text{Cov}(Z_{(k+1)\delta} - Z_{k\delta}, Z_\delta - Z_0) \\
&= \frac{1}{2} \text{Var}(Z_{(k+1)\delta} - Z_{k\delta}) - \text{Var}(Z_{k\delta} - Z_0) + \frac{1}{2} \text{Var}(Z_{(k-1)\delta} - Z_0).
\end{aligned}$$

**Proof.** First note that

$$\begin{aligned}
\text{Var}(Z_{(k+1)\delta} - Z_0) &= \text{Var}((Z_{(k+1)\delta} - Z_{k\delta}) + (Z_{k\delta} - Z_0)) \\
&= \text{Var}(Z_\delta - Z_0) + \text{Var}(Z_{k\delta} - Z_0) + 2\text{Cov}(Z_{(k+1)\delta} - Z_{k\delta}, Z_{k\delta} - Z_0).
\end{aligned}$$

By rearranging, we have

$$2\gamma_k^* \triangleq 2\text{Cov}(Z_{(k+1)\delta} - Z_{k\delta}, Z_{k\delta} - Z_0) = \text{Var}(Z_{(k+1)\delta} - Z_0) - \text{Var}(Z_\delta - Z_0) - \text{Var}(Z_{k\delta} - Z_0).$$

If  $k \geq 2$ , then

$$\begin{aligned}
2\gamma_k^* &= 2\text{Cov}(Z_{(k+1)\delta} - Z_{k\delta}, Z_{k\delta} - Z_0) \\
&= 2\text{Cov}(Z_{(k+1)\delta} - Z_{k\delta}, Z_{k\delta} - Z_\delta) + 2\text{Cov}(Z_{(k+1)\delta} - Z_{k\delta}, Z_\delta - Z_0) = 2\gamma_{k-1}^* + 2\gamma_k.
\end{aligned}$$

Hence,

$$\begin{aligned}
\gamma_k &= \frac{2\gamma_k^* - 2\gamma_{k-1}^*}{2} = \frac{1}{2} \left( \begin{array}{c} \text{Var}(Z_{(k+1)\delta} - Z_0) - \text{Var}(Z_\delta - Z_0) - \text{Var}(Z_{k\delta} - Z_0) \\ - (\text{Var}(Z_{k\delta} - Z_0) - \text{Var}(Z_\delta - Z_0) - \text{Var}(Z_{(k-1)\delta} - Z_0)) \end{array} \right) \\
&= \frac{1}{2} \text{Var}(Z_{(k+1)\delta} - Z_0) - \text{Var}(Z_{k\delta} - Z_0) + \frac{1}{2} \text{Var}(Z_{(k-1)\delta} - Z_0),
\end{aligned}$$

which is the required result. ■

Combining Lemma 1 and Theorem 1 gives us

$$\begin{aligned}
\gamma_k &= \frac{1}{2} (\text{Var}(P_{(k+1)\delta} - P_0) - 2\text{Var}(P_{k\delta} - P_0) + \text{Var}(P_{(k-1)\delta} - P_0)) \\
&= \frac{1}{2} (b(k+1)\delta + 2leb(A_{(k+1)\delta} \setminus A) - 2(bk\delta + 2leb(A_{k\delta} \setminus A)) + b(k-1)\delta + 2leb(A_{(k-1)\delta} \setminus A)) \kappa_2(L_1) \\
&= (leb(A_{(k+1)\delta} \setminus A) - 2leb(A_{k\delta} \setminus A) + leb(A_{(k-1)\delta} \setminus A)) \kappa_2(L_1),
\end{aligned}$$

$$\rho_k = \frac{\gamma_k}{\text{Var}(P_\delta - P_0)} = \frac{\text{leb}(A_{(k+1)\delta} \setminus A) - 2\text{leb}(A_{k\delta} \setminus A) + \text{leb}(A_{(k-1)\delta} \setminus A)}{b\delta + 2\text{leb}(A_\delta \setminus A)}.$$

■

**Proof of Corollary 1.** From Proposition 1 we have

$$\frac{\partial}{\partial t} \text{leb}(A_t \cap A) = -(d(-t) - b),$$

so mean value theorem states that, for any  $0 \leq t_1 < t_2 < t_3$ , there exist  $t_{23} \in (t_2, t_3)$  and  $t_{12} \in (t_1, t_2)$  such that

$$\begin{aligned} \frac{\text{leb}(A_{t_3} \cap A) - \text{leb}(A_{t_2} \cap A)}{t_3 - t_2} &= -(d(-t_{23}) - b) \\ &\leq -(d(-t_{12}) - b) \\ &= \frac{\text{leb}(A_{t_2} \cap A) - \text{leb}(A_{t_1} \cap A)}{t_2 - t_1}, \end{aligned} \tag{15}$$

where the second inequality follows from the monotonicity of  $d$  and  $t_{12} < t_{23}$ . This proves that  $\text{leb}(A_t \cap A)$  is a convex function of  $t$ . Hence, equation (2) implies

$$\begin{aligned} &\text{leb}(A_{(k+1)\delta} \setminus A) - 2\text{leb}(A_{k\delta} \setminus A) + \text{leb}(A_{(k-1)\delta} \setminus A) \\ &= -\text{leb}(A_{(k+1)\delta} \cap A) + 2\text{leb}(A_{k\delta} \cap A) - \text{leb}(A_{(k-1)\delta} \cap A) \leq 0, \end{aligned} \tag{16}$$

as required.

When  $d$  is a strictly increasing function, the inequality (15) becomes strict, so  $\text{leb}(A_t \cap A)$  becomes a strictly convex function of  $t$ , which further makes inequality (16) strict, as required. ■

**Proof of Theorem 4.** Arrivals are in  $D_t$  and so aggregated to  $\Sigma(D_t; r)$ , while departures only happen at most once due to the monotonicity of  $d$ . All the departures are in  $G_t$  and so aggregated to  $\Sigma(G_t; r)$ . Now

$$\begin{aligned} \mathbb{E}(\{P\}_t^{[r]}) &= \mathbb{E}(\Sigma(B_t; r)) + \mathbb{E}(\Sigma(H_t; r)) + \mathbb{E}(\Sigma(G_t; r)) \\ &= (\text{leb}(B_t) + \text{leb}(H_t) + \text{leb}(G_t)) \int_{-\infty}^{\infty} |y|^r \nu(dy) \\ &= (bt + (1-b)t + (1-b)t) \int_{-\infty}^{\infty} |y|^r \nu(dy) \\ &= (2-b)t \int_{-\infty}^{\infty} |y|^r \nu(dy), \end{aligned}$$

where the third equality follows from

$$\text{leb}(G_t) = \text{leb}(H_t \cup A) - \text{leb}(A_t) = \text{leb}(H_t) + \text{leb}(A) - \text{leb}(A_t) = \text{leb}(H_t) = (1-b)t.$$

■

**Proof of Proposition 2.** Stationarity of returns and the definition that  $\delta_n = T/n$  imply

$$\begin{aligned}\mathbb{E}\left(RV^{(n)}\right) &= \sum_{k=1}^n \mathbb{E}\left(P_{k\delta_n} - P_{(k-1)\delta_n}\right)^2 = n \text{Var}\left(P_{\delta_n} - P_0\right) + n\left(\mathbb{E}\left(P_{\delta_n} - P_0\right)\right)^2 \\ &= n(b\delta_n + 2leb(A_{\delta_n} \setminus A))\kappa_2(L_1) + n(b\delta_n\kappa_1(L_1))^2 \\ &= \left(b + 2\frac{leb(A_{\delta_n} \setminus A)}{\delta_n}\right)T\kappa_2(L_1) + b^2T\delta_n\kappa_1^2(L_1).\end{aligned}$$

■

**Details of Remark 11.** For any  $r \geq 0$  plug-in (13) into the left-hand side of (11). Then

$$\begin{aligned}(2-b) \sum_{y \in \mathbb{Z} \setminus \{0\}} |y|^r \widehat{\nu}(y) &= (2-b) \sum_{y \in \mathbb{Z} \setminus \{0\}} |y|^r \left( \frac{\hat{\alpha}_y - (1-b)\hat{\alpha}_{-y}\hat{\beta}_0}{(2-b)b} \right) \\ &= \frac{\sum_{y \in \mathbb{Z} \setminus \{0\}} |y|^r \hat{\alpha}_y - (1-b) \sum_{y \in \mathbb{Z} \setminus \{0\}} |y|^r \hat{\alpha}_{-y}\hat{\beta}_0}{b} = \sum_{y \in \mathbb{Z} \setminus \{0\}} |y|^r \hat{\alpha}_y \hat{\beta}_0,\end{aligned}$$

which has nothing to do with parameter  $b$ . ■

## B Computing probability mass functions of price changes

Let  $a_1, \dots, a_n$  be non-zero integers. We will demonstrate how the inverse fast Fourier transform (IFFT) can be used to calculate  $p_y \triangleq \mathbb{P}(Y = y)$  of  $Y \triangleq \sum_{k=1}^n a_k X_k \in \mathbb{Z}$ , where  $X_k$ 's are independent Poisson random variables with intensities  $\lambda_k$ .

The characteristic function of  $Y$  is:

$$\varphi(\theta \dagger Y) \triangleq \mathbb{E}\left(e^{i\theta Y}\right) = \mathbb{E}\left(e^{i\sum_{k=1}^n \theta a_k X_k}\right) = \prod_{k=1}^n \varphi(\theta a_k \dagger X_k) = \prod_{k=1}^n \exp\left(\lambda_k \left(e^{i\theta a_k} - 1\right)\right).$$

As  $Y$  is discrete, the discrete IFFT can be used to get  $p_y$ . Note that  $\varphi(\theta \dagger Y) = \sum_{y=-\infty}^{\infty} e^{i\theta y} p_y$ , so the inverse Fourier transform is justified by, for  $y = 0, 1, 2, \dots$ , as  $N \rightarrow \infty$ ,

$$\begin{aligned}\frac{1}{N} \sum_{k=0}^{N-1} \varphi\left(-\frac{2\pi k}{N} \dagger Y\right) e^{i2\pi ky/N} &= \frac{1}{N} \sum_{k=0}^{N-1} \sum_{y'=-\infty}^{\infty} p_{y'} e^{-i2\pi ky'/N} e^{i2\pi ky/N} \\ &= \frac{1}{N} \sum_{y'=-\infty}^{\infty} p_{y'} \sum_{k=0}^{N-1} e^{i2\pi k(y-y')/N} \rightarrow \sum_{y'=-\infty}^{\infty} p_{y'} 1_{\{y=y'\}} = p_y, \\ \frac{1}{N} \sum_{k=0}^{N-1} \varphi\left(\frac{2\pi k}{N} \dagger Y\right) e^{i2\pi ky/N} &= \frac{1}{N} \sum_{y'=-\infty}^{\infty} p_{y'} \sum_{k=0}^{N-1} e^{i2\pi k(y+y')/N} \rightarrow \sum_{y'=-\infty}^{\infty} p_{y'} 1_{\{y=-y'\}} = p_{-y},\end{aligned}$$

where the approximation here comes from the Riemann sum

$$\frac{1}{N} \sum_{k=0}^{N-1} e^{i2\pi k\theta'/N} = \int_0^1 e^{i2\pi\theta\theta'} d\theta + O(N^{-1}) = 1_{\{\theta'=0\}} + O(N^{-1}).$$

Hence, the IFFT will take the input of

$$\left( \varphi(0 \dagger Y), \varphi(-2\pi/N \dagger Y), \dots, \varphi\left(-\frac{2\pi(N-1)}{N} \dagger Y\right) \right)^T$$

and give the output as  $(p_0, \dots, p_{N-1})^T$  approximately; similarly, with the input of

$$\left( \varphi(0 \dagger Y), \varphi(2\pi/N \dagger Y), \dots, \varphi\left(\frac{2\pi(N-1)}{N} \dagger Y\right) \right),$$

the IFFT will give the output as  $(p_0, p_{-1}, \dots, p_{-(N-1)})^T$  approximately.

In Figure 10, we take  $N = 60$  in order to accurately compute  $p_y$  for  $y \in \{-30, \dots, 30\}$ .

## C Cleaning of the empirical data

Here we discuss the preprocessing procedures for the raw empirical data. For each data set, our database has the current bid price (`bid`), bid size (`bidsz`), ask price (`ask`), ask size (`asksz`), trade price (`trade`), trade volume (`tradesz`) and the record logging time on the data server (`log_t`). The following events will be logged into the raw data set chronologically:

1. A change of `bid` and `bidsz` (or `ask` and `asksz`), which will leave missing `ask`, `asksz` (or `bid`, `bidsz`), `trade` and `tradesz`.
2. A new instance of `trade` and `tradesz`, which will leave missing `bid`, `bidsz`, `ask` and `asksz`. This is usually followed by a record that shows the newest `bid` and `ask` status after the trading. Sometimes this updating record will be combined with its previous trading record.

**Step 1: Remove the wrong records (Optional).** We forward fill the missing values in columns `bid` and `ask`; after this, we examine whether the recorded trade price lies in the range from `bid` minus a factor `M` of tick sizes to `ask` plus `M` tick sizes. `M` here is manually chosen as 9.5 for the two EUC data sets, which is a conservative setting and will only remove those visually inspectable errors. We do not use this step for the two TNC data sets.

**Step 2: Preserve only the trading activities.** Since in this paper we are only concerned with the dynamics of the trade prices, we throw out all the other data records that are not directly associated with a trade, that is, those rows with missing `trade` and `tradesz`.

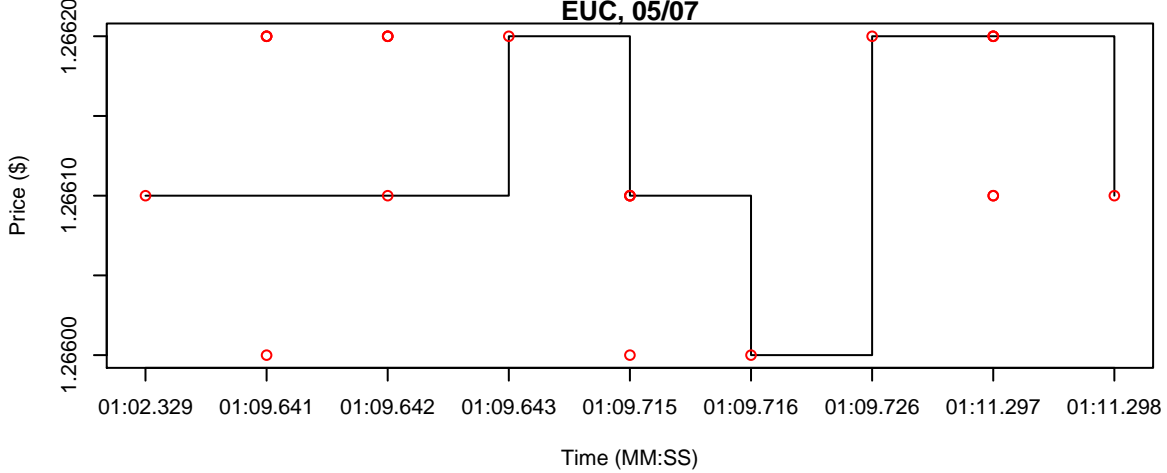


Figure 12: An illustration of the definition of a unique price when multiple data records share the same time tag. The white points illustrate all the trade prices appeared in the data with the same time tag; the black solid line represent the unique price we define. This data is EUC1006 between 00:01:02 and 00:01:12 on May 7. Code: `Price_Plots.R`.

**Step 3-1: Associate a unique price to a time tag.** Occasionally several data feeds will be pushed into the data server almost at the same time but perhaps with different prices. Then we iteratively define a unique price for this particular time tag by the price that is closest to the price of the previous time tag. Figure 12 illustrates this.

**Step 3-2: Do nothing for an ambiguous case.** If it happens that there are exactly two trade prices with the same time tag that are just one tick above and one tick below the previous price—which we call an ambiguous case (e.g. at time 01:09.641 in Figure 12), then we will use the previous price as the price for the current time tag.

**Step 4: Keep only jumps.** For our analysis it is sufficient to keep only the columns `Time` and `Price`, such that `Time` is always increasing without duplicates while `Price` have no two adjacent elements that take the same value. `Price` is always the value the price process takes immediately after a jump.

## D Non-parametric inference of the trawl function

Let  $\tilde{d}(s)$  be the *non-squashed trawl function* with  $\tilde{d}(-\infty) = 0$  such that  $d(s) \triangleq b + (1 - b)\tilde{d}(s)$ . Then equation (2) implies  $\partial_\delta \text{leb}(A_\delta \setminus A) = (1 - b)\tilde{d}(-\delta)$ . Hence,

$$\frac{\partial \widehat{\sigma}_\delta^2}{\partial \delta} = \left( \frac{b + 2(1 - b)\tilde{d}(-\delta)}{2 - b} \right) \sum_{y \in \mathbb{Z} \setminus \{0\}} y^2 \hat{\alpha}_y \hat{\beta}_0, \quad \frac{\partial \widehat{\sigma}_\delta^2}{\partial \delta}(\infty) = \left( \frac{b}{2 - b} \right) \sum_{y \in \mathbb{Z} \setminus \{0\}} y^2 \hat{\alpha}_y \hat{\beta}_0,$$

which then gives us

$$b = \frac{2 \left( \widehat{\partial_\delta \sigma_\delta^2} \right) (\infty)}{\left( \widehat{\partial_\delta \sigma_\delta^2} \right) (0) + \left( \widehat{\partial_\delta \sigma_\delta^2} \right) (\infty)}, \quad \tilde{d}(-\delta) = \frac{\widehat{\partial_\delta \sigma_\delta^2} - \left( \widehat{\partial_\delta \sigma_\delta^2} \right) (\infty)}{\left( \widehat{\partial_\delta \sigma_\delta^2} \right) (0) - \left( \widehat{\partial_\delta \sigma_\delta^2} \right) (\infty)},$$

where  $\left( \widehat{\partial_\delta \sigma_\delta^2} \right) (0) = \sum_{y \in \mathbb{Z} \setminus \{0\}} y^2 \hat{\alpha}_y \hat{\beta}_0$ . Therefore, by estimating  $\widehat{\partial_\delta \sigma_\delta^2}$  for every  $\delta$  the trawl function is revealed non-parametrically.

In practice, it might be demanding to get  $\left( \widehat{\partial_\delta \sigma_\delta^2} \right) (\infty)$ , the asymptotic slope of the sample variogram  $\widehat{\sigma_\delta^2}$  against  $\delta$ , because as  $\delta$  being larger, the sample size we use to calculate  $\widehat{\sigma_\delta^2}$  is getting smaller. Is it possible to use other moment equations in Theorem 1 to identify  $b$  rather than through the boundary behavior of  $\widehat{\partial_\delta \sigma_\delta^2}$  for  $\delta \rightarrow \infty$ ? Unfortunately, the answer is no.  $b$  and  $d$  are not identifiable if we neither parameterize  $d$  nor adopt a boundary estimation for  $b$  at  $\delta \rightarrow \infty$ .

To justify this point, assume that one wants to employ all the other additional moment equations in Theorem 1 to identify  $b$ :

$$\begin{aligned} \kappa_j (P_\delta - P_0) &= \left( b\delta + \left( 1 + (-1)^j \right) \text{leb} (A_\delta \setminus A) \right) \kappa_j (L_1) \\ &= \left( b\delta + \left( 1 + (-1)^j \right) \text{leb} (A_\delta \setminus A) \right) \sum_{y \in \mathbb{Z} \setminus \{0\}} y^j \nu(y), \quad j \geq 3. \end{aligned}$$

Denote the sample  $j$ -th cumulant with sampling interval  $\delta$  as  $\widehat{\kappa}_{j,\delta}$ . Then equation (13) implies that

$$\begin{aligned} \frac{\partial \widehat{\kappa}_{j,\delta}}{\partial \delta} &= \left( b + \left( 1 + (-1)^j \right) \frac{\partial}{\partial \delta} \text{leb} (A_\delta \setminus A) \right) \sum_{y \in \mathbb{Z} \setminus \{0\}} y^j \frac{\hat{\alpha}_y - (1-b) \hat{\alpha}_{-y}}{(2-b)b} \hat{\beta}_0 \\ &= \left( b + \left( 1 + (-1)^j \right) (1-b) \tilde{d}(-\delta) \right) \frac{\sum_{y \in \mathbb{Z} \setminus \{0\}} y^j \hat{\alpha}_y - (1-b) \sum_{y \in \mathbb{Z} \setminus \{0\}} y^j \hat{\alpha}_{-y}}{(2-b)b} \hat{\beta}_0 \\ &= \left( b + \left( 1 + (-1)^j \right) (1-b) \tilde{d}(-\delta) \right) \frac{1 - (-1)^j (1-b)}{(2-b)b} \sum_{y \in \mathbb{Z} \setminus \{0\}} y^j \hat{\alpha}_y \hat{\beta}_0 \\ &= \begin{cases} \sum_{y \in \mathbb{Z} \setminus \{0\}} y^j \hat{\alpha}_y \hat{\beta}_0 & , \text{ for } j \text{ odd} \\ \frac{\widehat{\partial \sigma_\delta^2} / \partial \delta}{\sum_{y \in \mathbb{Z} \setminus \{0\}} y^2 \hat{\alpha}_y \hat{\beta}_0} \sum_{y \in \mathbb{Z} \setminus \{0\}} y^j \hat{\alpha}_y \hat{\beta}_0 & , \text{ for } j \text{ even} \end{cases} , \end{aligned}$$

which is still again independent of  $b$ .